




ARTICLE

Disruption of *mosGILT* in *Anopheles gambiae* impairs ovarian development and *Plasmodium* infection

Jing Yang^{1*}, Tyler R. Schleicher^{1*}, Yuemei Dong², Hyun Bong Park^{3,4}, Jiangfeng Lan⁵, Peter Cresswell^{6,7} , Jason Crawford^{3,4,8} , George Dimopoulos^{2**}, and Erol Fikrig^{1,9**} 

***Plasmodium* infection in *Anopheles* is influenced by mosquito-derived factors. We previously showed that a protein in saliva from infected *Anopheles*, mosquito gamma-interferon-inducible lysosomal thiol reductase (*mosGILT*), inhibits the ability of sporozoites to traverse cells and readily establish infection of the vertebrate host. To determine whether *mosGILT* influences *Plasmodium* within the mosquito, we generated *Anopheles gambiae* mosquitoes carrying mosaic mutations in the *mosGILT* gene using CRISPR/CRISPR associated protein 9 (Cas9). Here, we show that female mosaic *mosGILT* mutant mosquitoes display defects in ovarian development and refractoriness to *Plasmodium*. Following infection by either *Plasmodium berghei* or *Plasmodium falciparum*, mutant mosquitoes have significantly reduced oocyst numbers as a result of increased thioester-containing protein 1 (TEP1)-dependent parasite killing. Expression of vitellogenin (Vg), the major yolk protein that can reduce the parasite-killing efficiency of TEP1, is severely impaired in mutant mosquitoes. *MosGILT* is a mosquito factor that is essential for ovarian development and indirectly protects both human and rodent *Plasmodium* species from mosquito immunity.**

Introduction

Malaria remains one of the greatest threats to human health, accounting for over 200 million cases and approximately half a million deaths each year (World Health Organization, 2017). *Plasmodium* parasites, the causative agents of malaria, require the *Anopheles* mosquito for their sporogonic development and transmission to vertebrates. The parasite life cycle in the mosquito begins when *Plasmodium* gametocytes differentiate into gametes in the midgut lumen. Fusion of male and female gametes produces zygotes, which develop into motile ookinetes within 12–20 h. After traversing the midgut epithelium, the ookinetes transform into oocysts at the basal lamina. Mature oocysts burst and release sporozoites into the hemocoel. The sporozoites that successfully invade the salivary glands (SG) are ready to be transmitted to a new host (Ghosh et al., 2000; Sinden, 2002).

Mosquitoes mount potent immune responses against *Plasmodium* development between the ookinete and oocyst stages, causing substantial losses in parasite numbers (Blandin and Levashina, 2004; Christophides et al., 2002; Dimopoulos et al., 1998, 2002; Sinden, 2002). Thioester-containing protein

1 (TEP1), a complement-like glycoprotein, is one of the key anti-parasitic immune effectors in mosquitoes (Blandin et al., 2004; Levashina et al., 2001). The direct binding of TEP1 to the surface of ookinetes targets the parasites for destruction by lysis or melanization (Blandin et al., 2004). Silencing of *TEP1* enhances *Plasmodium berghei* oocyst numbers and abolishes parasite melanization in both the susceptible and refractory strains of *Anopheles gambiae* (Blandin et al., 2004; Collins et al., 1986; Povelones et al., 2011). In addition, positive regulators of this complement-like immunity have been identified, including two members of the leucine-rich repeat immune protein (LRIM) family, LRIM1 (Fraiture et al., 2009; Osta et al., 2004; Povelones et al., 2009) and APL1C (Fraiture et al., 2009; Povelones et al., 2009; Riehle et al., 2006, 2008), and the CLIP-domain serine protease homologue SPCLIP1 (Dong et al., 2006; Povelones et al., 2013). These mosquito immune factors constitute defense mechanisms that restrict or eliminate *Plasmodium* development.

There are also a variety of mosquito factors that repress the immune responses, thereby promoting the development and

¹Section of Infectious Diseases, Department of Internal Medicine, Yale University School of Medicine, New Haven, CT; ²Department of Molecular Microbiology and Immunology, Bloomberg School of Public Health, Johns Hopkins University, Baltimore, MD; ³Department of Chemistry, Yale University, New Haven, CT; ⁴Chemical Biology Institute, Yale University, West Haven, CT; ⁵College of Fisheries, Huazhong Agricultural University, Wuhan, China; ⁶Department of Immunobiology, Yale University School of Medicine, New Haven, CT; ⁷Department of Cell Biology, Yale University School of Medicine, New Haven, CT; ⁸Department of Microbial Pathogenesis, Yale University School of Medicine, New Haven, CT; ⁹Howard Hughes Medical Institute, Chevy Chase, MD.

*J. Yang and T.R. Schleicher contributed equally to this paper; **G. Dimopoulos and E. Fikrig contributed equally to this paper; Correspondence to Erol Fikrig: erol.fikrig@yale.edu; George Dimopoulos: gdimopo1@jhu.edu.

© 2019 Yang et al. This article is distributed under the terms of an Attribution–Noncommercial–Share Alike–No Mirror Sites license for the first six months after the publication date (see <http://www.rupress.org/terms/>). After six months it is available under a Creative Commons License (Attribution–Noncommercial–Share Alike 4.0 International license, as described at <https://creativecommons.org/licenses/by-nc-sa/4.0/>).

subsequent transmission of *Plasmodium* (Blandin et al., 2008; Simões et al., 2018). *A. gambiae* (Ag) C-type lectin (CTL) 4 and CTL mannose binding 2 were shown to protect *P. berghei* and *Plasmodium falciparum* ookinetes from melanization in susceptible mosquitoes (Osta et al., 2004; Simões et al., 2017). Mosquito serpin SRPN2 is another *Plasmodium* agonist in *A. gambiae*, which facilitates ookinete invasion of the midgut by inhibiting lysis and melanization (Michel et al., 2005). Two nutrient transport proteins, lipophorin (Lp) and vitellogenin (Vg), reduce the parasite-killing efficiency of TEP1 (Rono et al., 2010). However, most studies have used the rodent parasite *P. berghei* as a model. Specific mosquito factors that promote the development of human malaria parasites remain to be identified.

Previously, we identified a protein, mosquito IFN- γ -inducible lysosomal thiol reductase (mosGILT), that binds to sporozoites in the saliva of infected *Anopheles* mosquitoes (Schleicher et al., 2018). We showed that mosGILT can partially reduce the speed and cell traversal activity of both human and rodent *Plasmodium* sporozoites. The inhibition of these motility components impairs the ability of the sporozoites to migrate to the liver and establish a normal hepatic infection. To determine whether mosGILT influences *Plasmodium* infection in mosquitoes, we generated mosaic *mosGILT*-mutant mosquitoes using CRISPR/CRISPR-associated protein 9 (Cas9), a powerful technique that enables the study of mosquito gene function through efficient genome editing (Dong et al., 2018). Here we show that *A. gambiae* mosquitoes carrying mosaic mutations in the *mosGILT* gene show defects in ovarian development. These mutant mosquitoes have markedly lower numbers of oocysts, following infection by either rodent or human malaria parasites (*P. berghei* or *P. falciparum*). This leads to a dramatic decrease in sporozoite load and infection of the SGs. The refractory phenotype of *mosGILT* mutant mosquitoes is strongly associated with their reduced expression of Vg, which leads to a more efficient TEP1-mediated killing of ookinetes. Therefore, mosGILT is a mosquito factor that plays an important role in ovarian development and indirectly protects both human and rodent *Plasmodium* species from mosquito immunity.

Results

Generation of mosaic *mosGILT* mutant mosquitoes

To generate *mosGILT*-deficient mosquitoes, we first created a transgenic line expressing three guide RNAs (gRNAs) targeting the *mosGILT* gene (Fig. 1 a) based on an established CRISPR/Cas9 system in *A. gambiae* (Dong et al., 2018). Heterozygous females of the gRNA-expressing line were crossed with homozygous males of the *vasa-Cas9* strain (Gantz et al., 2015; Hammond et al., 2016). Progeny from this cross were separated by fluorescent markers into two groups: the *gRNA-RFP⁺/Cas9-GFP⁺* transheterozygotes and the *gRNA-RFP⁻/Cas9-GFP⁺* siblings (referred to as siblings; Fig. S1 a). In 100% of the *gRNA/Cas9* transheterozygotes ($n > 40$), Cas9 induced polymorphic mutations at the gRNA1- and gRNA3-target sites, but not the gRNA2-target site (Fig. 1 b). Our previous study showed that mosGILT is an abundant protein in *A. gambiae* SGs (Schleicher et al., 2018). Endogenous SG mosGILT in female *gRNA/Cas9* transheterozygotes was greatly reduced compared

with that of siblings (Fig. 1 c). These data suggest that CRISPR/Cas9-mediated disruption of *mosGILT* is highly efficient in *gRNA/Cas9* transheterozygotes (referred to as *mosGILT* mutants), which is consistent with a previous study showing that the *vasa* promoter-driven Cas9 is ubiquitously expressed in both the germ line and somatic cells (Port et al., 2014).

Next, we sought to obtain homozygous *mosGILT* knockout mosquitoes by crossing the *mosGILT* mutants with the X1 line (Voloehonsky et al., 2015). However, all progeny (51 out of 51) from *mosGILT* mutant males crossed with X1 females only carried WT *mosGILT* alleles, and none of the *mosGILT* mutant females (0 out of 48) were able to lay eggs after mating with X1 males (Fig. S1 a). These results indicate that the disruption of *mosGILT* interferes with both male and female mosquito reproductive biology. In addition, crossing of heterozygous *mosGILT*-gRNA₃-expressing males with homozygous *vasa-Cas9* females produced fewer eggs compared with the reciprocal cross, and all the hatched progeny were *gRNA-RFP⁻/Cas9-GFP⁺* (Fig. S1 b). We hypothesize that maternal deposition of Cas9 in the embryo allows an earlier disruption of *mosGILT*, causing embryonic lethality. Together, these data suggest that homozygous *mosGILT* knockout mosquitoes cannot be obtained as the mutations are not heritable. Therefore, we used the F₀ mosaic *mosGILT* mutants as a model for further study.

MosGILT mutant mosquitoes show severe defects in ovarian development

MosGILT mutants survived from larvae to adulthood with a normal lifespan, wing length, feeding propensity, and sex ratio (female:male, 1.15:1), with only a slightly delayed pupation time compared with siblings (Fig. S2 a). Their inability, however, to pass down the mutated alleles of *mosGILT* prompted us to examine the gonads. Morphological analysis showed that 100% of the female mutants ($n > 90$) had underdeveloped ovaries that were completely devoid of follicles, whereas their SGs appeared normal (Fig. 2 a). Yolk accumulation and oocyte development were not observed in any of the abnormal ovaries after blood feeding, and their median size was significantly smaller than that of siblings (Fig. 2, b and c). These data suggest that *mosGILT* plays a critical role in ovarian development. In line with this, we found that there were detectable levels of *mosGILT* expression in the ovaries of WT females, in addition to the fat body and SGs (Fig. S2 b). Furthermore, we detected *mosGILT* expression in WT larvae and pupae (Fig. S2 c). Additionally, we found that 100% of the *mosGILT* mutant males ($n > 70$) displayed developmental defects of the testes (Te), although their male accessory glands appeared to be normal (Fig. S2 d). These data indicate that *mosGILT* is expressed in different tissues and developmental stages, and therefore could have multiple *in vivo* functions. As only the female mosquitoes take blood meals and are responsible for malaria transmission, we further analyzed the female *mosGILT* mutants.

Plasmodium infection is impaired in *mosGILT* mutant mosquitoes

To assess the effect of *mosGILT* disruption on *Plasmodium* infection in the vector, we first fed the female *mosGILT* mutants on

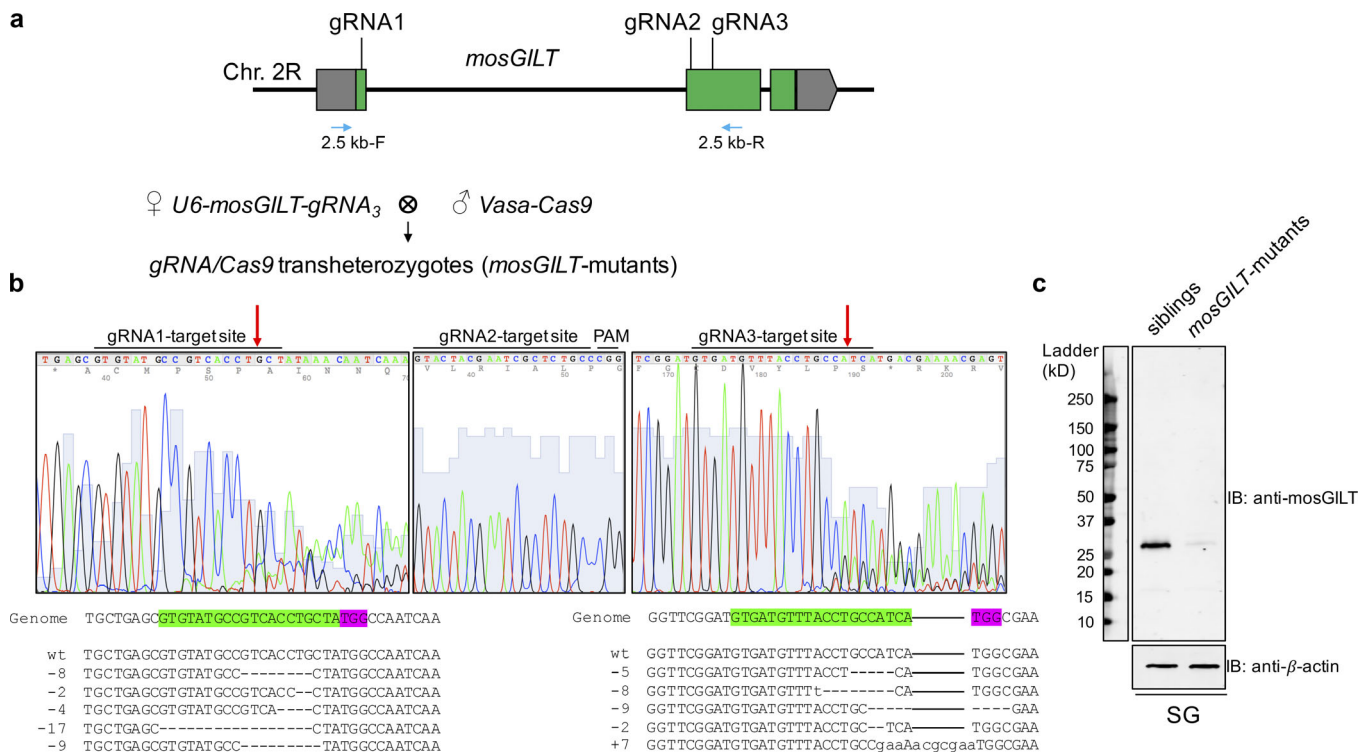


Figure 1. Generation of mosaic *mosGILT* mutant mosquitoes using CRISPR/Cas9. (a) Schematic of gRNA target sites at the *mosGILT* locus. Coding sequences are shown in green blocks. Untranslated regions are shown in gray. Blue arrows indicate the positions of primers (2.5 kb-F and 2.5 kb-R; Table S1) used for PCR amplification of the gRNA-target regions. (b) Examples of sequencing results of Cas9-induced mutations in *mosGILT* mutant mosquitoes. The 2.5 kb PCR products from individual *mosGILT* mutants ($n > 40$) were sequenced and showed similar results. Multiple peaks begin at the Cas9 cutting site (3 nt upstream of the PAM, red arrows) in both the gRNA1- and gRNA3-target regions (left and right panels, respectively; PAM sequences are masked by mutations). Examples of sequences of the gRNA1- or gRNA3-target locus in mosaic mutant mosquitoes revealed frame-shift mutations, in-frame mutations, and WT sequence. No mutations were detected in the gRNA2-target region (middle panel; intact PAM is indicated). (c) Western blots of SGs from *mosGILT* mutant mosquitoes and siblings. Five mosquitoes were used per lane. Blots were probed with monoclonal mouse anti-*mosGILT* and monoclonal mouse anti- β -actin as a loading control at 1:1,000 dilutions. Chr, chromosome; IB, immunoblotting.

mice infected with the rodent malaria parasite *P. berghei*, using siblings as the control. *MosGILT* mutants displayed a significant reduction in the oocyst infection intensity at 8 d post-infection (dpi), compared with siblings (Fig. 3 a; siblings, $n = 50$, median = 81; and *mosGILT* mutants, $n = 50$, median = 0; 100% reduction in median; $P < 0.0001$, Mann-Whitney test). Midgut infection prevalence (the percentage of infected midguts with at least one oocyst) in *mosGILT* mutants was 34.1%, a significant 2.3-fold decrease from 77.8% in siblings (Fig. 3 b; $P < 0.0001$, Fisher's exact test). Consistently, *mosGILT* mutants had a significantly lower number of SG sporozoites at 21 dpi compared with siblings (Fig. 3 c; siblings, $n = 10$, median = 16,263; and *mosGILT* mutants, $n = 10$, median = 1,009; 93.8% reduction in median; $P = 0.0001$, Mann-Whitney test). The SG infection prevalence (the percentage of infected SG) in *mosGILT* mutants was 12.6%, fivefold lower than 62.9% in siblings (Fig. 3 d; $P < 0.0001$, Fisher's exact test).

Next, we examined the permissiveness of *mosGILT* mutants to the human malaria parasite, *P. falciparum*. The oocyst infection intensity of *mosGILT* mutants was significantly lower than that of siblings (Fig. 3 e; siblings, $n = 104$, median = 9; and *mosGILT* mutants, $n = 88$, median = 4.5; 50% reduction in median; $P < 0.0001$, Mann-Whitney test). In addition, the midgut infection prevalence of *mosGILT* mutants was 72.3%, compared with 93.2%

in siblings (Fig. 3 f; $P < 0.0001$, Fisher's exact test). The number of SG sporozoites was greatly reduced in *mosGILT* mutants compared with siblings (Fig. 3 g; siblings, $n = 63$, median = 5,813; and *mosGILT* mutants, $n = 63$, median = 1,688; 71% reduction in median; $P < 0.0001$, Mann-Whitney test). The SG infection prevalences in *mosGILT* mutants and siblings were 63.9% and 90.5%, respectively (Fig. 3 h; $P = 0.0005$, Fisher's exact test). Together, these results demonstrate that *mosGILT* disruption compromises *Plasmodium* infection in *A. gambiae* mosquitoes.

Disruption of *mosGILT* increases TEP1-dependent parasite killing

TEP1 is one of the key *Anopheles* immune effectors involved in the elimination of invading ookinetes, through lysis and/or melanization (Blandin et al., 2004; Dong et al., 2006; Fraiture et al., 2009; Povelones et al., 2011, 2013; Volohonsky et al., 2017). Therefore, we examined whether the suppression of *Plasmodium* by *mosGILT* disruption requires TEP1. *TEP1* mRNA levels were greatly reduced (>85%) in siblings and *mosGILT* mutants injected with *TEP1* double-stranded RNA (dsRNA) compared with control mosquitoes injected with luciferase (*luc*) dsRNA (Fig. 4 a). Strikingly, both siblings and *mosGILT* mutant mosquitoes showed a similar level of significantly increased numbers of *P.*

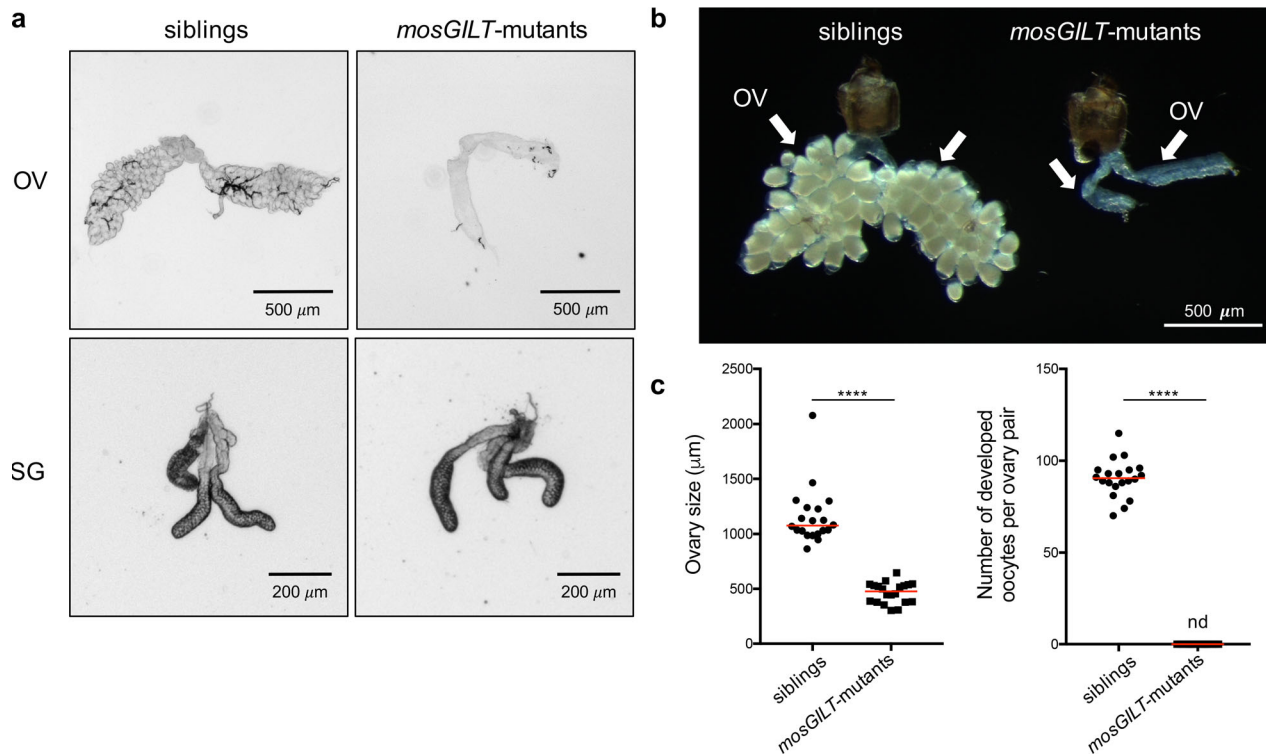


Figure 2. Ovarian development is blocked in *mosGILT* mutant mosquitoes. (a) Ovaries (OV) and SGs dissected from female *mosGILT* mutants and siblings (scale bars, 500 μm for ovaries, 200 μm for SG). (b) Ovary (white arrows) dissected from female mosquitoes 48 h after blood feeding (scale bar, 500 μm). All images are representative pictures of tissues collected from > 30 mosquitoes. (c) Ovary size (left) and oocyte number per ovary pair (right) from female siblings and *mosGILT* mutants at 48 h after blood feeding. Each dot represents the data from one mosquito ($n = 20$ /group, Mann–Whitney test, ****, $P < 0.0001$, nd not detected). The horizontal lines (red) indicate the medians.

berghei oocysts upon *TEP1* silencing (Fig. 4 b). The percentages of infected midguts in both siblings and *mosGILT* mutants reached 100% when *TEP1* was depleted (Fig. 4 c). These results suggest that the parasite loss in *mosGILT* mutants was dependent on the *TEP1*-mediated immune response.

In addition, our immunofluorescence assay showed a significant reduction of early oocysts in the midgut epithelium of *mosGILT* mutants compared with siblings at 48 h post-infection (hpi; Fig. 4, d and e). Very few ookinetes were observed in both groups, probably because most of them had been cleared by the *TEP1*-dependent immune response by that time point. Consistent with a previous study (Blandin et al., 2004), we also observed a weak and patchy binding pattern of *TEP1* to some early oocysts, whereas the dying or dead ookinetes were heavily coated by *TEP1* (Fig. 4 d). Furthermore, melanized ookinetes were hardly seen in the *P. berghei*-infected midguts 8 dpi from both siblings and *mosGILT* mutants, whereas silencing of *CTLA*, a negative regulator of melanization (Osta et al., 2004; Simões et al., 2017), triggered ookinete melanization in siblings (Fig. S3). Together, these data imply that *TEP1*-mediated lysis, but not melanization, is responsible for limiting parasite survival in *mosGILT* mutant mosquitoes.

Underdeveloped ovaries compromise the expression of 20-hydroxyecdysone (20E) and Vg in *mosGILT* mutants

To understand how *mosGILT* disruption influences the *TEP1*-dependent responses, we analyzed the mRNA and protein

levels of *TEP1* in *mosGILT* mutants and siblings. At 24 hpi, transcripts of *TEP1* were up-regulated at similar levels in the fat body from both groups of mosquitoes (Fig. 5 a). The full-length form of *TEP1* (*TEP1*-FL) is secreted into the hemolymph and processed into the mature C-terminal fragment (*TEP1*-C; Fraiture et al., 2009; Levashina et al., 2001; Povelones et al., 2009). Hemolymph analysis by immunoblotting did not reveal any obvious difference in the amounts of *TEP1*-FL or *TEP1*-C between *mosGILT* mutants and siblings (Fig. 5 b). These results suggest the expression and activation of *TEP1* are not altered by *mosGILT* disruption.

Vg is a precursor protein of egg yolk that is mainly synthesized in the female fat body and provides nutrients for oogenesis in the ovaries, a process known as vitellogenesis (Attardo et al., 2005). Vg has also been shown to reduce the parasite-killing efficiency of *TEP1* (Rono et al., 2010). Considering the abnormal ovaries and increased *TEP1*-dependent responses in *mosGILT* mutants, we investigated whether Vg expression was impaired in the absence of *mosGILT*. To assess this, we analyzed the mRNA and protein levels of Vg in *mosGILT* mutants and siblings. Transcripts of Vg were significantly up-regulated in the fat body of siblings after taking an infectious blood meal; however, Vg induction was severely impaired in *mosGILT* mutants (Fig. 5 a). Vg protein in the hemolymph can be readily visualized by Coomassie staining of SDS-PAGE gels (Rono et al., 2010). Using this approach, we further validated that the protein level of Vg

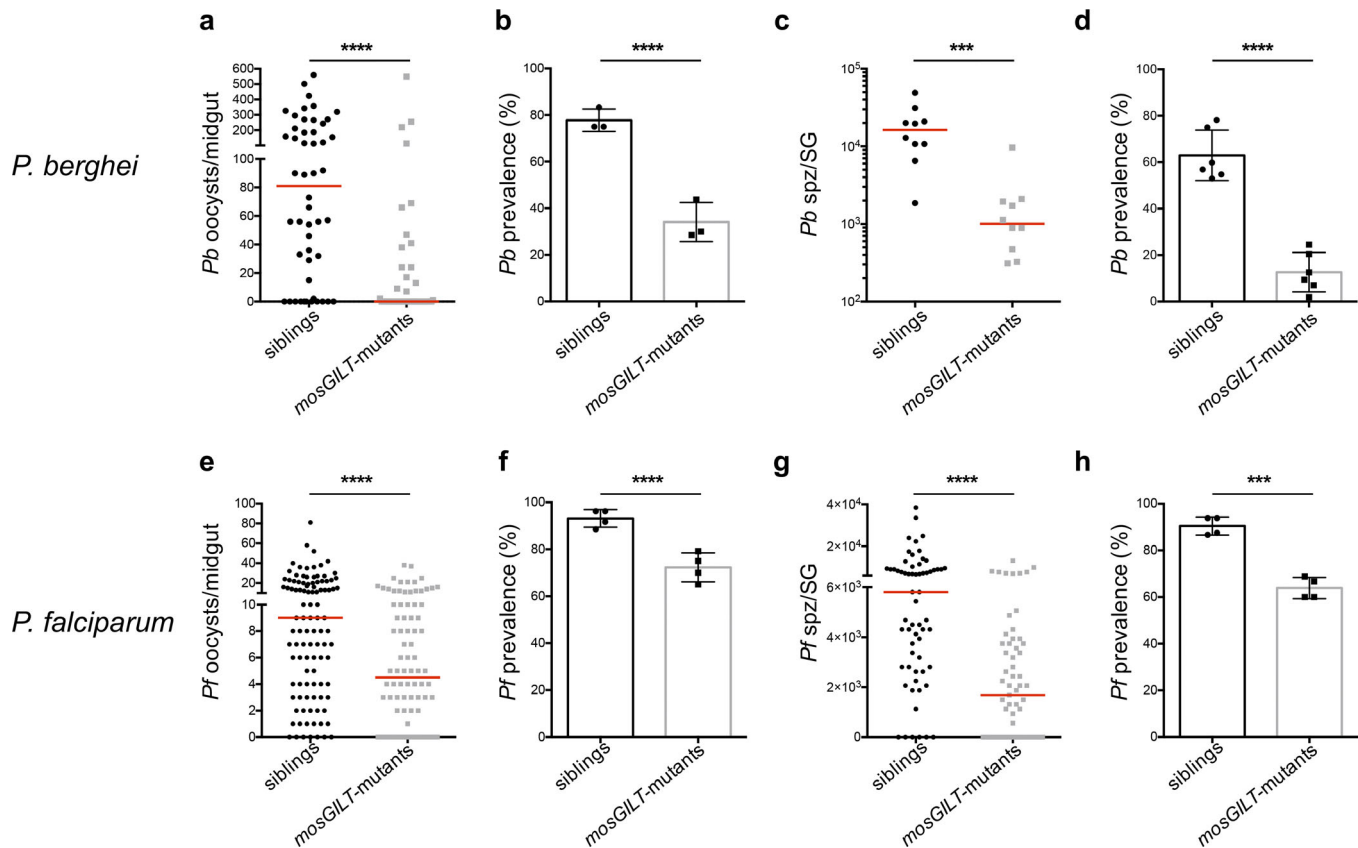


Figure 3. *Plasmodium* infection is impaired in *mosGILT* mutant mosquitoes. (a–d) *P. berghei* (*Pb*) infection intensities in *mosGILT* mutant mosquitoes and siblings. *P. berghei* oocyst number (a) and infection prevalence (b) in the midgut 8 dpi. Each dot in panel a represents the oocyst number in one mosquito midgut (data pooled from three independent experiments, $n = 50$ /group, Mann–Whitney test, **, $P < 0.0001$). *P. berghei* sporozoite number (c) and infection prevalence (d) in the SGs 21 dpi. Each dot in panel c represents the average number of sporozoites from five siblings or 10 *mosGILT* mutant mosquitoes, respectively (data pooled from three independent experiments, $n = 10$ /group, Mann–Whitney test, ***, $P = 0.0001$). (e–h) *P. falciparum* (*Pf*) infection intensities in *mosGILT* mutant mosquitoes and siblings. *P. falciparum* oocyst number (e) and infection prevalence (f) in the midgut 8 dpi. Each dot in panel e represents the oocyst number in one mosquito midgut (data pooled from four independent experiments, siblings $n = 104$, *mosGILT* mutants $n = 88$, Mann–Whitney test, ****, $P < 0.0001$). *P. falciparum* sporozoite number (g) and infection prevalence (h) in the SGs 14 dpi. Each dot in panel g represents the sporozoite number from one mosquito (data pooled from four independent experiments, $n = 63$ /group, Mann–Whitney test, ****, $P < 0.0001$). The horizontal lines (red) indicate the medians. In the infection prevalence assays, each dot represents one independent experiment (mean \pm SD, Fisher’s exact test, ***, $P = 0.005$, ****, $P < 0.0001$). Spz, sporozoites.**

was also greatly reduced in *mosGILT* mutants compared with siblings at 24 hpi (Fig. 5 b).

In mosquitoes, a blood meal triggers the ovaries to secrete ecdysone, an insect steroid hormone, which is converted to 20E that in turn activates Vg production in the fat body (Gabrieli et al., 2014; Hagedorn et al., 1975; Pondeville et al., 2008; Raikhel et al., 2005). Using an enzyme immunoassay (EIA) kit, we found that the amount of 20E induced by blood feeding was significantly lower in *mosGILT* mutants compared with siblings (Fig. 5 c). This result further indicates that the underdeveloped ovaries fail to function properly, causing the impaired production of 20E and the downstream synthesis of Vg.

Complementation of 20E rescues the Vg expression and *P. berghei* infection in *mosGILT* mutants

In addition to the impaired 20E production, *mosGILT* mosaic mutations might cause additional defects that lead to the reduction of Vg and parasites. To address this possibility, exogenous 20E was supplied to female mutants. First, we found that Vg

expression in blood-fed *mosGILT* mutants was rescued by 20E in a dose-dependent manner (Fig. S4), indicating that Vg synthesis in the fat body, a downstream event in the 20E signaling pathway, is not affected by *mosGILT* disruption. The amount of exogenous 20E required for optimal Vg induction in *mosGILT* mutants was 0.5–1.0 $\mu\text{g}/\text{female}$, similar to the doses used for artificial stimulation of vitellogenesis in sugar-fed *Aedes aegypti* mosquitoes (Lea, 1982). Next, we examined the effects of 20E complementation on *P. berghei* infection. The Vg expression, oocyst number, and midgut infection prevalence were all significantly enhanced in the 20E-injected *mosGILT* mutants compared with noninjected controls (Fig. 6). In addition, these parameters were not significantly different between the 20E-injected *mosGILT* mutants and the 20E-injected siblings (Fig. 6). Furthermore, we found that silencing of *mosGILT* in WT females, which have already developed normal ovaries, did not affect Vg expression or *P. berghei* infection (Fig. S5). Together, these data suggest that lack of 20E due to the underdeveloped ovaries is the main factor contributing to the Vg reduction and refractoriness to *P. berghei* in *mosGILT* mutants.

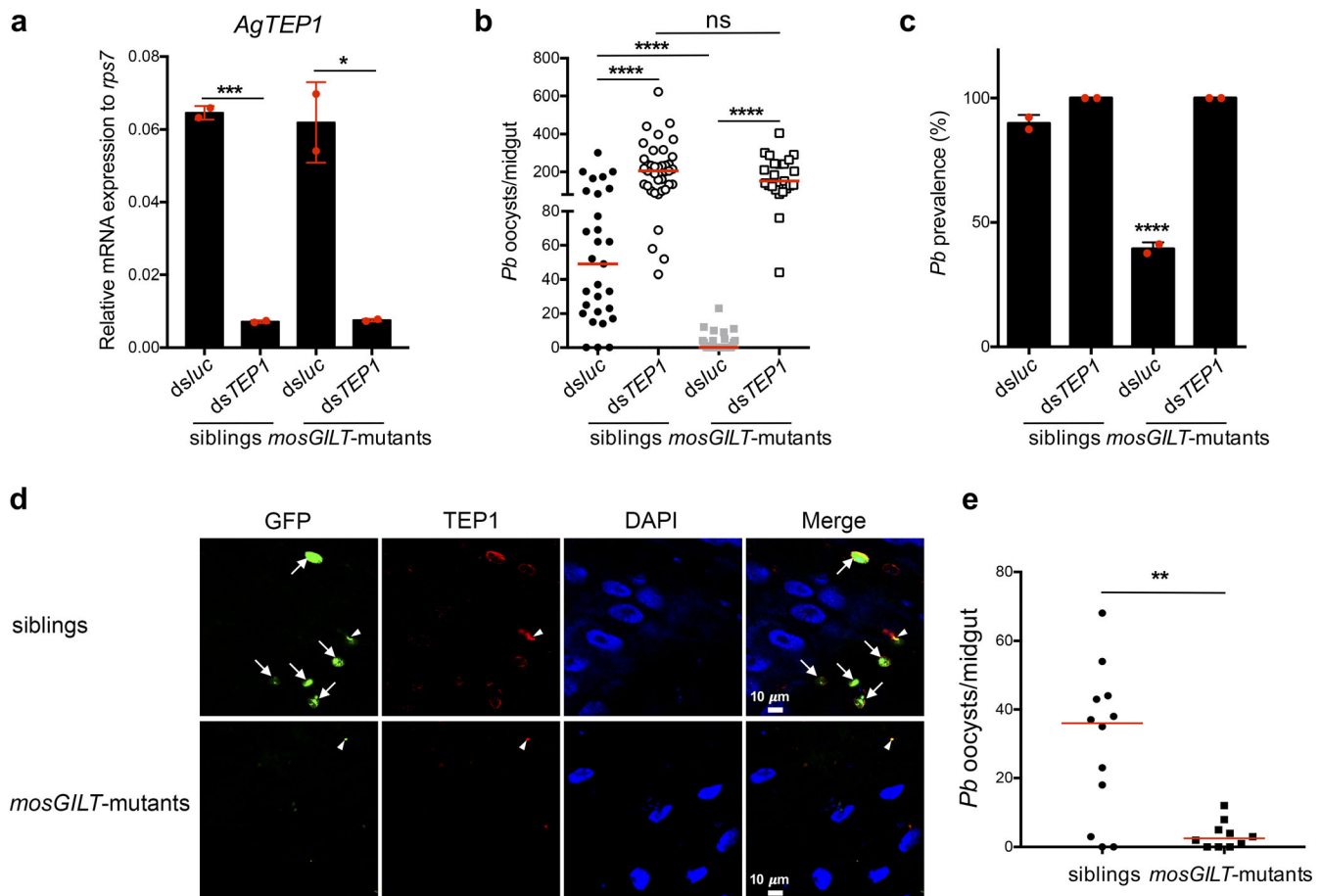


Figure 4. The refractoriness of *mosGILT* mutant mosquitoes to *P. berghei* infection is dependent on the TEP1-mediated immune response. (a) Knockdown efficiency of *A. gambiae* (*Ag*) *TEP1* was validated by RT-qPCR of fat body cells 4 d after dsRNA injection. Data are representative of more than three experiments (each dot represents five mosquitoes, mean \pm SD, unpaired t test, *, $P < 0.05$, ***, $P < 0.001$). **(b and c)** *P. berghei* (*Pb*) oocyst number (b) and infection prevalence (c) in the midgut 8 dpi. Each dot in panel b represents the oocyst number in one mosquito midgut (data pooled from two independent experiments, siblings *dsLuc* $n = 29$, siblings *dsTEP1* $n = 39$, *mosGILT* mutants *dsLuc* $n = 33$, *mosGILT* mutants *dsTEP1* $n = 23$, Mann-Whitney test, ****, $P < 0.0001$, ns, not significant). The horizontal lines (red) indicate the medians. Each dot in panel c represents one independent experiment (mean \pm SD, Fisher's exact test, ****, $P < 0.0001$). **(d)** Immunostaining of *P. berghei* parasites (green) and TEP1 (red) in the midguts at 48 hpi (scale bars, 10 μ m). Arrows indicate early oocysts. Arrowheads indicate dying or dead ookinetes. Nuclei of mosquito midgut cells were stained with DAPI. All images are representative pictures of infected midguts from at least 10 mosquitoes in each group. **(e)** Quantification of early oocyst numbers in panel d. Data are representative of three independent experiments (siblings $n = 12$, *mosGILT* mutants $n = 10$, Mann-Whitney test, **, $P < 0.01$).

Discussion

The trade-off between reproduction and immunity has been documented in diverse insect species (Schwenke et al., 2016). Understanding the molecular mechanisms linking reproduction and immunity in *Anopheles* mosquitoes is of significant importance for developing malaria control strategies. Two nutrient transport proteins in *A. gambiae*, Lp, and Vg, have been shown to interfere with anti-*Plasmodium* responses after taking an infectious blood meal (Mendes et al., 2008; Rono et al., 2010; Vlachou et al., 2005). Using CRISPR/Cas9-generated mosaic *mosGILT* mutant mosquitoes, we now uncover a critical role for *mosGILT* in mosquito ovary development and *Plasmodium* survival in the midgut. In this study, female *mosGILT* mutant mosquitoes displayed underdeveloped ovaries after eclosion and reproductive defects including severely impaired production of 20E and Vg. In addition, the *mosGILT* mutant mosquitoes mounted a notably stronger TEP1-mediated immune response against developing

ookinetes in the midgut, resulting in a lower susceptibility to infection by either *P. berghei* or *P. falciparum*. Our results provide new evidence that mosquito proteins involved in reproduction can benefit malaria parasite infection in the vector by suppressing immunity.

We demonstrate the application of CRISPR/Cas9 in a mosaic analysis of *mosGILT* functions in *A. gambiae*. Genome editing in embryos using CRISPR/Cas9 often results in genetic mosaicism in founder animals (F_0), which can be used as models for phenotyping especially when a homozygous gene knockout is developmentally lethal (Mianné et al., 2017; Port et al., 2014; Song et al., 2018). A previous study of CRISPR tools in *Drosophila* has shown that *vasa-Cas9* in combination with *U6-gRNA* allows efficient biallelic gene disruption, which could readily reveal null mutant phenotypes in the soma (Port et al., 2014). Consistent with these reports, we found that 100% of the F_0 *mosGILT* mutants generated by crossing *vasa-Cas9* males with *U6-mosGILT*-

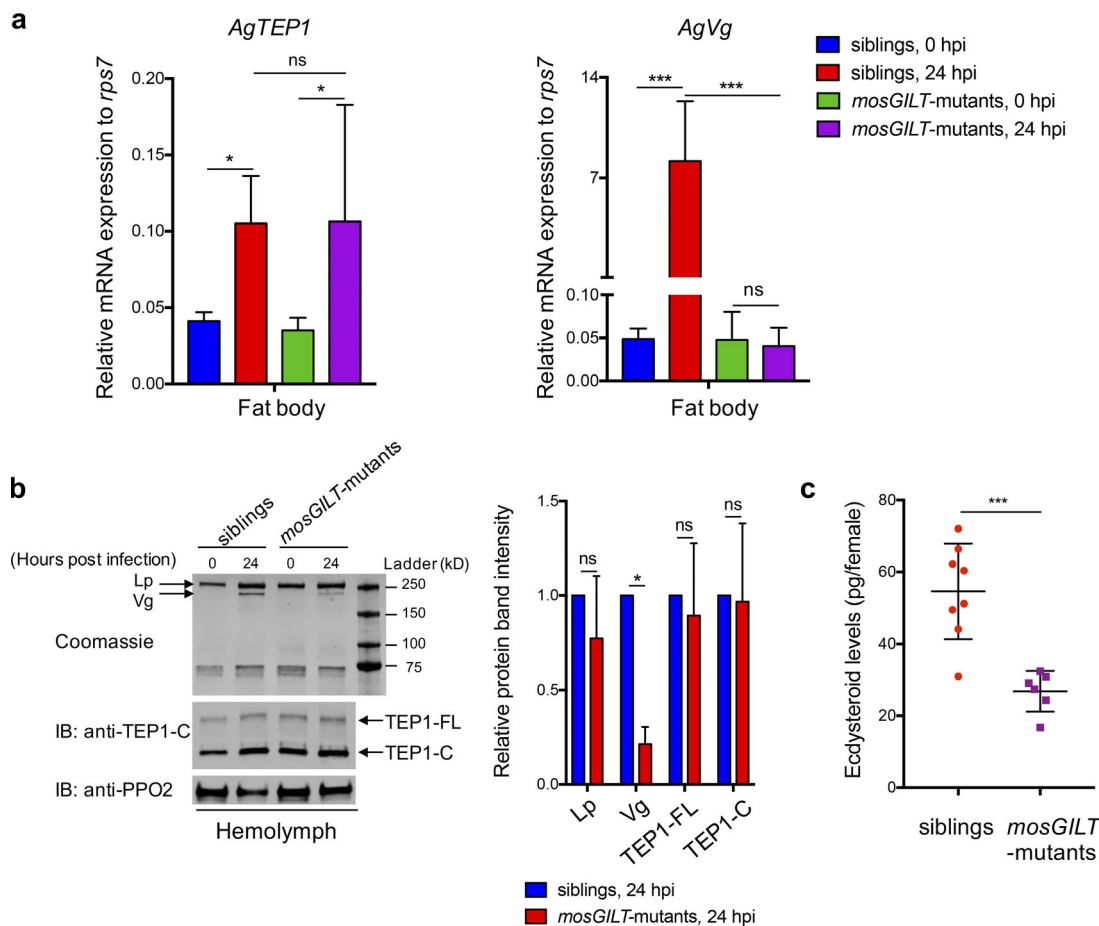


Figure 5. **MosGILT is required for normal expression of Vg.** (a) Transcript levels of *AgTEP1* and *AgVg* in the female fat body at 0 and 24 h after feeding on *P. berghei*-infected mice. Data represent duplicate experiments from two experiments (mean \pm SD, one-way ANOVA, uncorrected Fisher's least significant difference, *, $P < 0.05$, ***, $P = 0.0001$, ns, not significant). (b) Western blots and SDS-PAGE of hemolymph from *mosGILT* mutants and siblings at 0 and 24 h after feeding on *P. berghei*-infected mice. Blots (left) were probed with polyclonal rabbit anti-TEP1 (1:200), and polyclonal rabbit anti-PPO2 (1:15,000) as a loading control. TEP1-FL and TEP1-C are indicated. Lp and Vg protein levels in hemolymph were visualized by Coomassie staining. Band intensities (Lp, Vg, TEP1-FL, and TEP1-C) for *mosGILT* mutants 24 hpi were quantified by densitometry from two independent experiments and normalized to the PPO2 signal. Data are presented as relative band signal intensity (right) compared with siblings 24 hpi (mean \pm SD, two-way ANOVA, *, $P < 0.05$, ns, not significant). (c) Ecdysteroid levels in siblings and *mosGILT* mutants, 24 h after feeding on *P. berghei*-infected mice, were measured using an EIA kit. Data are representative of two independent experiments (each dot represents one mosquito, siblings $n = 8$, *mosGILT* mutants $n = 6$, mean \pm SD, unpaired *t* test, ***, $P = 0.0005$).

gRNA₃ females were genetic mosaics. They carried diverse *mosGILT* mutations (Fig. 1 b). More importantly, *mosGILT* mutant females had a greatly reduced *mosGILT* protein level in the SGs (Fig. 1 c) and displayed abnormal ovaries (Fig. 2). In addition, *mosGILT* is probably also essential for embryogenesis, as the reciprocal cross using homozygous *vasa*-Cas9 females and heterozygous *U6-gRNA* males produced only WT mosquitoes (Fig. S1 b). We speculate that a higher maternal supply of Cas9 in the egg allows the mutagenesis of *mosGILT* to occur at an earlier time point, which results in embryonic lethality.

When female *Anopheles* mosquitoes acquire a blood meal infected with *Plasmodium*, they not only initiate egg development in the ovaries but also allow the parasite to infect the midgut. The nutrients in the blood trigger the ovaries to produce ecdysone, an insect steroid hormone, which is converted to 20E and initiates vitellogenesis in the fat body (Baldini et al., 2013; Hagedorn et al., 1975; Kokoza et al., 2001). Vg, one of the yolk protein precursors, is highly induced during vitellogenesis and

essential for oogenesis (Attardo et al., 2005). The abnormal ovaries in *mosGILT* mutant mosquitoes were unable to develop follicles (Fig. 2) or produce 20E (Fig. 5 c) in response to a blood meal, resulting in the subsequent loss of Vg production (Fig. 5) and egg development (Fig. 2, b and c; and Fig. S1 a). In addition to the severe defects in ovary function, *mosGILT* mutant mosquitoes showed a strong refractoriness to malaria infection. *P. berghei* oocyst number and infection prevalence were significantly lower in *mosGILT* mutants compared with siblings (Fig. 3, a and b). Of the few surviving oocysts in the *mosGILT* mutants, we did not observe a striking difference in their size compared with that of siblings (Fig. S3), and we showed that *TEP1* silencing strongly reversed the phenotype (Fig. 4, b and c). Therefore, we believe that the low permissiveness of *mosGILT* mutant mosquitoes to *P. berghei* was mostly the result of *TEP1*-mediated immunity. *TEP1* expression and cleavage were not altered by *mosGILT* disruption (Fig. 5); however, we observed a significant loss of oocysts by 48 dpi, likely due to more efficient killing of

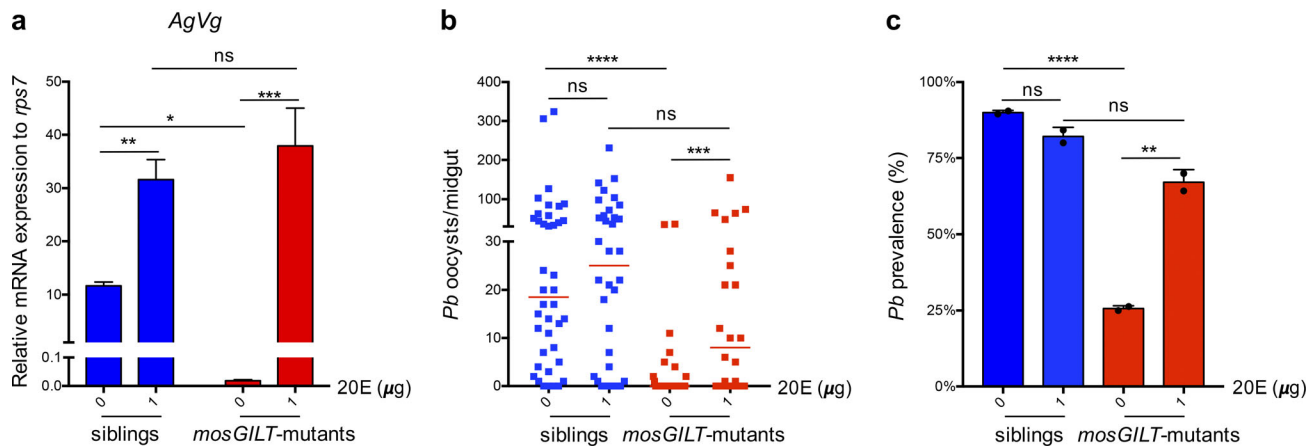


Figure 6. Complementation of exogenous 20E rescues the Vg expression and *P. berghei* infection in *mosGILT* mutants. (a) Transcript levels of *AgVg* in the fat body of females at 24 hpi. 20E was injected into mosquitoes at 2 hpi. Data are representative of three independent experiments (mean \pm SD, one-way ANOVA, uncorrected Fisher's least significant difference, *, $P < 0.05$, **, $P < 0.01$, ***, $P < 0.001$, ns, not significant). (b and c) *P. berghei* oocyst number (b) and infection prevalence (c) in the midgut of females at 8 dpi. 20E was injected into mosquitoes at 2 hpi. Each dot in panel b represents the oocyst number in one mosquito midgut (data pooled from two independent experiments, $n = 40, 34, 35,$ and 24 for the four groups of mosquitoes, Mann-Whitney test, ***, $P < 0.001$, ****, $P < 0.0001$, ns, not significant). The horizontal lines (red) indicate the medians. Each dot in panel c represents one independent experiment (mean \pm SD, Fisher's exact test, **, $P < 0.01$, ****, $P < 0.0001$, ns, not significant).

parasites by TEPI in *mosGILT* mutants (Fig. 4, d and e). A previous study has shown that *Vg* silencing decreased *P. berghei* survival by increasing the binding efficiency of TEPI to ookinetes (Rono et al., 2010). Considering the low *Vg* production due to underdeveloped ovaries in *mosGILT* mutants, here we also observed a strong positive correlation between the *Vg* level and *P. berghei* oocyst number. More importantly, the refractory phenotype of *mosGILT* mutants extended to the human malaria species, *P. falciparum* (Fig. 3, e and f), which is consistent with a previous finding that TEPI can limit *P. falciparum* infection in *A. gambiae* (Dong et al., 2006).

A recent publication demonstrated that steroid hormone signaling influences *Plasmodium* development in *Anopheles* (Werling et al., 2019). The authors generated transgenic *A. gambiae* females by inducing mutagenesis in the *zero population growth* (*zpg*) gene, which has been shown to be essential for germ cell development (Tazuke et al., 2002; Thailayil et al., 2011). Similar to the phenotypes that we found in *mosGILT* mutants, the Δzpg mutant females also showed underdeveloped ovaries that produced low amounts of 20E, and were significantly less permissive to *P. falciparum* infection. Both mutant mosquito models reveal a positive link between 20E signaling and intensity of *Plasmodium* infection. Consistent with this idea, complementation of exogenous 20E to *mosGILT* mutants rescued the infection by *P. berghei* (Fig. 6, b and c). Therefore, we propose that *mosGILT* benefits *Plasmodium* survival by influencing ovarian development and the subsequent production of 20E and *Vg*.

Previously, we reported a negative role of SG *mosGILT* in the transmission of *Plasmodium* sporozoites to the mammalian host (Schleicher et al., 2018). In contrast, here we describe a positive role of *mosGILT* in ovarian development and *Plasmodium* survival in the midgut. These different findings could be attributed to diverse functions of *mosGILT* at various developmental stages

and distinct tissue localizations (Fig. S2). In addition, although we initially showed that *mosGILT* does not have thiol reductase activity in an in vitro assay at pH 4.0 compared with mammalian GILT proteins (Schleicher et al., 2018), we cannot completely exclude the possibility that *mosGILT* has some reducing activity in vivo. Any putative enzymatic activity of *mosGILT* and its role in ovarian development still require further investigation. It is possible that *mosGILT* directly or indirectly influences ovarian development by regulating the local redox conditions before the adult stage. Identification of the *mosGILT* interactome and the implicated signaling pathways would further our understanding of *mosGILT* in vivo functions. Additionally, it would be interesting to examine whether *mosGILT* homologues in other insect species play similar roles in ovarian development and pathogen transmission.

Vector reproduction intimately interacts with immune defense pathways, as these two processes are simultaneously initiated after a blood meal. Identification of vector proteins involved in the cross-talk between reproduction and immunity could provide new targets for the development of disease-control strategies. Our study demonstrates a critical role of *mosGILT* in the reproduction of *A. gambiae* mosquitoes. Particularly, disruption of *mosGILT* in females impairs the development and function of ovaries, leading to increased anti-*Plasmodium* immunity. These findings can potentially lead to new preventive strategies for malaria, aimed at inhibiting the activity of *mosGILT* to induce mosquito sterility and reduce the vectorial capacity of *A. gambiae*.

Materials and methods

Ethics statement

Mice were housed by the Yale Animal Resource Center at Yale University and handled under the Guide for the Care and Use of

Laboratory Animals of the National Institutes of Health. The animal experimental protocol was approved by the Institutional Animal Care and Use Committee of Yale University (protocol permit no. 2017-07941). Human blood for *P. falciparum* cultures and mosquito infections was collected from a pool of pre-screened donors under an institutional review board-approved protocol at Johns Hopkins University (protocol NA00019050).

gRNA target design

Putative gRNA sequences targeting the first and second exons of the *mosGILT* gene were identified using online tools such as ZiFit and CRISPR Design. gRNA sequences were required to be 20 nucleotides in length, start with a guanine to facilitate transcription by the U6 promoter, and be followed by a protospacer adjacent motif (PAM; NGG, where N is any nucleotide). Three gRNA sequences that had the fewest predicted genomic off-targets were selected (Table S1).

Generation of gRNA constructs

Plasmids expressing *mosGILT*-gRNAs were constructed as previously described (Dong et al., 2018). In brief, linear double-stranded DNA fragments encoding each gRNA were produced by annealing two partially overlapping oligos (primers *mosGILT*-gRNA1-F and -R for gRNA1, *mosGILT*-gRNA2-F and -R for gRNA2, *mosGILT*-gRNA3-F and -R for gRNA3; Table S1). To generate pKSB-gRNA modules (pKSB-*mosGILT*-gRNA-1, -2, -3), the three double-stranded DNA fragments were individually cloned into a pBluescript vector backbone that contained the U6 snRNA polymerase III promoter (AGAP013557), CRISPR RNA invariable sequences, and the RNA polIII TTTT terminator. The pKSB-gRNA modules were used to assemble the three gRNA genes into the pDSAR vector via the Golden Gate assembly system (E1600S; NEB) for embryo microinjection into the *A. gambiae* docking line X1 (Vолоhonsky et al., 2015). The backbone plasmid pDSAR with 3xP3-RFP allowed screening of gRNA-positive larvae or mosquitoes by red fluorescence in the eyes.

Embryo microinjection and generation of gRNAs transgenic mosquito line

Embryo microinjection and screening of positive gRNA-expressing lines were performed as previously described (Dong et al., 2018). A QIAGEN Endofree Maxi Kit was used to prepare pDSAR-*mosGILT*-gRNA₃ and a helper plasmid containing the *vasa2::ΦC31 integrase* gene (pENTR-R4R3-*vasa2*-integrase; Papathanos et al., 2009; Волоhonsky et al., 2015). The gRNA plasmid (160 ng/μl) and the helper plasmid (200 ng/μl) in a phosphate buffer (0.1 mM NaHPO₄ buffer, and 5 mM KCl, pH 6.8) were microinjected into 580 embryos of the docking strain X1 (Meredith et al., 2013; Волоhonsky et al., 2015). Injected eggs were maintained on wet filter paper for 2 d before hatching. 15% of the injected eggs hatched, and 32% of the survived G₀ larvae showed RFP signals at the second instar larval stage. RFP-positive G₀ pupae were sexed (14 females and 12 males) and then organized into two cohorts. G₀ female mosquitoes were crossed with WT X1 male mosquitoes at a ratio of 1:1, and G₀ male mosquitoes were crossed with female X1 mosquitoes at a ratio of 1:5. The G₁ progeny were examined for RFP-

glowing eyes at both the larval and adult stages. Positive G₁ mosquitoes were outcrossed with X1 for two generations followed by two generations of self-crossing to enrich the homozygous mosquitoes by the screening of RFP in the larvae before crossing with the *vasa*-Cas9 strain to generate the *mosGILT* mutants.

Generation of *mosGILT* mutant mosaic mosquitoes

The G₄ gRNA-expressing mosquitoes were crossed with the homozygous Cas9 transgenic strain (*vasa2*-Cas9; with green fluorescence in the eyes; Hammond et al., 2016). 100 *mosGILT*-gRNA female mosquitoes were crossed with 100 male Cas9 mosquitoes to generate the *mosGILT* mutant mosquitoes. Since the parental gRNA mosquitoes were not fully homozygous, the progeny of this cross were separated into two groups by screening the RFP signal at the larvae stage: the group of larvae with both RFP and GFP signals was *gRNA/Cas9* transgenic, and the other group of larvae carrying only the *Cas9-GFP* transgene serves as a negative control (referred to as siblings). Pupae or adult mosquitoes were randomly selected from the *gRNA/Cas9* transgenic group for genomic DNA extraction using the DNEasy Blood and Tissue Kit (69581; QIAGEN). The gRNA-targeted genomic locus was amplified by PCR with flanking primers (2.5 kb-F and -R; Table S1). PCR products were separated with an agarose gel (1%). The WT 2.5 kb bands were purified by DNA gel extraction (QIAGEN) and cloned using pCR2 TOPO-cloning system (Thermo Fisher Scientific). Individual clones were sent for DNA sequencing to confirm any Cas9-mediated mutations at the gRNA-targeted region. Due to the ubiquitous expression of Cas9 driven by the *vasa* promoter (Port et al., 2014), all *gRNA/Cas9* transgenic mosquitoes are mosaic mutants that contain mixed genotypes with different mutations at the *mosGILT* gene locus throughout their tissues. The SGs of *mosGILT* mutant mosaic mosquitoes were dissected for Western blot analysis to confirm the reduction of *mosGILT* expression compared with the sibling mosquitoes.

Animals

All the *A. gambiae* mosquito lines were derived from the G3 strain, including the docking line X1 (Vолоhonsky et al., 2015), *vasa2*-Cas9 (Hammond et al., 2016), *mosGILT*-gRNA₃, *mosGILT* mutant and sibling mosquitoes. They were raised at 27°C, 80% humidity, under a 12/12 h light/dark cycle and maintained with 10% sucrose. Swiss Webster mice (6–8-wk-old females) were purchased from Charles River Laboratories.

Fitness measurements of adult mosquitoes

After *mosGILT*-gRNA female mosquitoes were crossed with Cas9 male mosquitoes, the offspring larvae were maintained according to a standard procedure with 400 larvae per tray (Pike et al., 2017). For pupation time measurement, pupae were collected and screened under the fluorescent microscope to record the number of *mosGILT* mutant pupae (GFP⁺/RFP⁺) and their siblings (GFP⁺/RFP⁻) on a daily basis.

To examine the morphology of ovaries, SGs, and Te, at least 30 female or male mosquitoes from the *mosGILT* mutant and sibling group were anesthetized on ice and dissected.

Representative pictures of ovaries and SGs from unfed mosquitoes were captured using an EVOS FL Auto Cell Imaging System (Thermo Fisher Scientific). Representative pictures of ovaries from blood-fed mosquitoes were taken with a Zeiss Discovery V8 stereomicroscope using a Zeiss camera AxioCam MRc equipped with AxionVision 4.8 software.

To test the ability of male mutants to pass down the mutated *mosGILT* gene, 50 *mosGILT* mutant male mosquitoes were crossed with 50 female X1 mosquitoes. 51 offspring were used for genomic DNA extraction. The gRNA-targeted genomic locus was amplified by PCR with flanking primers (2.5 kb-F and -R; Table S1), and PCR products were sent for sequencing as mentioned above.

For the fecundity assay of female mosquitoes, 50 female mosquitoes from both the mutant and the sibling groups were mated with 50 male X1 mosquitoes respectively for 4 d and then fed on naive 6–8-wk-old female Swiss Webster mice (Charles River Laboratories). Only the fed mosquitoes were selected for further analysis. 3 d after feeding, 25 female mosquitoes from each group were individually placed into *Drosophila* vials (AS574; Thermo Fisher Scientific) containing a conical filter paper surrounding the plastic wall and 1 cm of deionized water to lay eggs. Two days later, dead mosquitoes were excluded, and the number of mosquitoes in each group that laid eggs was recorded.

***P. berghei* infection**

P. berghei (ANKA GFPcon 259cl2, MRA-865; ATCC) was maintained as previously described (Schleicher et al., 2018). In brief, 6–8-wk-old female Swiss Webster mice (Charles River Laboratories) were infected with parasitized mouse blood by needle injection. 5 d later, mice with parasitemia levels between 1% and 10% were used to feed mosquitoes that were deprived of sucrose for 20 h (3–5 mice/cage of 200 mosquitoes). The blood-fed mosquito cages were kept hydrated with damp paper towels at 20°C. 2 d after feeding, bottles containing a cotton wick soaked in 10% sucrose supplemented with 0.5% penicillin/streptomycin were provided to the remaining mosquitoes and subsequently changed every 3 d. 7–10 dpi, mosquitoes were anesthetized on ice, and the presence of GFP-expressing oocysts in their midguts was screened under a fluorescent microscope. 18–21 dpi, the presence of GFP-expressing sporozoites in the SGs was screened using a fluorescent microscope.

***P. falciparum* infection**

A. gambiae mosquitoes were starved for 3–5 h and then fed on NF54 *P. falciparum* gametocyte cultures (NF54: BEI Resources, MRA-1000; mature gametocytes were adjusted to 0.02% in 40% human red blood cells [O⁺] containing 60% heat-inactivated human serum [O⁺]; please refer to the ethics statement) through artificial membranes at 37°C at the Johns Hopkins Malaria Institute Core Facility as previously described (Angleró-Rodríguez et al., 2016; Dong et al., 2018; Trager and Jensen, 1976). Unfed mosquitoes were removed immediately after blood feeding, and the remaining mosquitoes were incubated at 27°C for 8 d to check oocysts in the midgut, or 14 d to check sporozoites in the SGs.

Parasite counts

P. berghei-infected midguts were dissected 8 dpi, stained with 0.2% mercurochrome (M7011; Sigma-Aldrich) in PBS, and examined using a ZEISS Axio Scope A1 optical microscope equipped with a Zeiss camera AxioCam MRc 5 and ZEN 2011 (blue edition) software in bright-field under a 5× objective. Images were imported into ImageJ (v1.49), and the numbers of live oocysts and melanized ookinetes were counted manually. For *P. berghei* sporozoite counting, infected SGs were dissected into 100 μl PBS. Then sporozoites were released from the SGs by repeated passaging through a 28 1/2-gauge insulin syringe (10 times). The sporozoite SG mixture was filtered through a 40-μm cell strainer (352340; Falcon) and centrifuged at 17,200 ×g for 10 min. The sporozoite pellet was resuspended in 30 μl of PBS and counted using a hemocytometer.

P. falciparum-infected midguts were dissected 8 dpi, stained with 0.2% mercurochrome (M7011; Sigma-Aldrich) in PBS, and examined using a phase-contrast microscope (Leica) as previously described (Dong et al., 2018). At least two to three biological replicates were performed for each experiment. For *P. falciparum* sporozoite counting, SGs were dissected and individually placed in 30 μl of PBS, followed by homogenization on ice. 10 μl of this homogenate was placed in a Neubauer counting chamber and counted after 5 min using a Leica phase-contrast microscope at 400× magnification.

Hemolymph collection

Mosquitoes were anesthetized on ice and kept on a cold glass slide with their ventral side up. The proboscis was clipped using dissection scissors, and the lateral aspects of the thorax were gently pressed by fine forceps to force out a visibly clear drop of hemolymph from the cut proboscis (Povelones et al., 2009). Hemolymph droplets from 15 mosquitoes were collected into 15-μl Laemmli sample buffer using a pipette tip. Proteins in the hemolymph were separated by SDS-PAGE and analyzed by Coomassie staining or Western blot. Each lane was loaded with hemolymph collected from 10 mosquitoes.

Immunostaining

P. berghei-infected mosquitoes were dissected 48 hpi. The midgut was cut open along its length to remove the bulk of the blood meal and then fixed in 4% paraformaldehyde in PBS for 45 min at room temperature. After washing three times with PBS, midguts were blocked in PBS with 1% BSA and 0.05% Triton X-100 for 4 h at room temperature, followed by incubation with rabbit polyclonal anti-TEP1-C antibody (1:300; Fraiture et al., 2009) overnight at 4°C. They were then washed three times with PBS containing 0.05% Triton X-100 and incubated with goat anti-rabbit Alexa Fluor 555 secondary antibody (1:500; A-21428; Thermo Fisher Scientific) overnight at 4°C. Midguts were washed as before, and stained with monoclonal anti-GFP antibody (1:250; A-11120; Thermo Fisher Scientific) and a goat anti-mouse Alexa Fluor 488 secondary antibody (1:500; A-11029; Thermo Fisher Scientific), mounted with Prolong Gold Antifade containing DAPI (Thermo Fisher Scientific), and monitored using a Leica SP5 confocal microscope. Three replicates of at least

10 midguts from *mosGILT* mutant and sibling mosquitoes were analyzed. Images were processed using ImageJ (v1.49).

Gene expression

Tissues (SGs, midguts, ovaries, or fat bodies) from 5 mosquitoes, 5–10 larvae, or 5–10 pupae were dissected into an RLT buffer (a guanidine-thiocyanate-containing lysis buffer), and total RNA was extracted using an RNeasy Mini Kit (QIAGEN). cDNA was made with an iScript kit (Bio-Rad) following the manufacturer's protocol. Quantitative PCR was performed using iQ SYBR Green Supermix (Bio-Rad) on a CFX96 real-time system (Bio-Rad) as previously described (Schleicher et al., 2018). The relative expression of different mosquito genes was normalized to *A. gambiae* ribosomal protein *s7* (*rps7*; primers in Table S1) using the comparative Ct method (Livak and Schmittgen, 2001).

Western blotting

Proteins were resolved by SDS-PAGE using 4–20% Mini-Protein TGX gels (Bio-Rad) at 300 V for 20 min and then transferred onto a 0.2- μ m nitrocellulose membrane for 60 min at 80 V in a Tris-Glycine transfer buffer with 25% methanol. Blots were blocked in 5% nonfat milk in PBS containing 0.1% Tween-20 for 30 min at room temperature. Primary antibodies were diluted in blocking buffer and incubated with the blots for 1 h at room temperature or 4°C overnight (4C10G9 mouse anti-*mosGILT* monoclonal 1:1,000, 0.8 μ g/ml; mouse anti- β actin monoclonal, Abcam 8224, 1:1,000; rabbit anti-TEP1 polyclonal 1:200, and rabbit anti-prophenoloxidase 2 [PPO2] polyclonal 1:15,000, two kind gifts from Dr. Elena A. Levashina, Vector Biology Unit, Max Planck Institute for Infection Biology, Berlin, Germany). Infra-red fluorescent secondary antibodies, goat anti-mouse IRDye 680LT (926-68020; LI-COR), or goat anti-rabbit IRDye 800CW (926-32211; LI-COR) was diluted in blocking buffer at 1:5,000 and incubated for 1 h at room temperature. Blots were washed in PBS with 0.1% Tween-20 three times for 5 min and then imaged with a LI-COR Odyssey Fc imaging system. Gel densitometry was performed using the in-built quantification tools on the LI-COR Odyssey Fc imaging system and normalized to the PPO2 signal. Data are presented as relative band signal intensity comparing the *mosGILT* mutants to siblings.

Gene silencing

RNA interference was performed as previously described (Povelones et al., 2011; Schleicher et al., 2018). dsRNA targeting *mosGILT*, *TEP1*, *CTLA*, or an irrelevant *luc* gene from *Renilla reniformis* (Schleicher et al., 2018), were transcribed using the MEGAScript RNAi kit (Thermo Fisher Scientific, Ambion; primers in Table S1).

2-d-old *A. gambiae* mosquitoes were injected with dsRNA using a Nanoject II Auto-Nanoliter Injector (Drummond) and allowed to recover in paper cups with 10% sucrose for 2 d. For silencing of *CTLA* or *TEP1*, 0.35 μ g of total dsRNA was used for each mosquito. For silencing of *mosGILT*, 1.0 μ g of total dsRNA was injected into each mosquito. On day 4 after dsRNA injection, these mosquitoes were deprived of sucrose for 20 h before allowing them to feed on *P. berghei*-infected mice with 3–5% parasitemia. Unfed mosquitoes were immediately discarded,

and the fed remaining mosquitoes were maintained with 10% sucrose containing 0.05% penicillin/streptomycin for 8 d at 20°C. On day 8 after infection, oocysts and melanized ookinetes in the midgut were counted as mentioned above.

Ecdysteroid quantification

Ecdysteroid titers were determined by a 20E EIA kit (Cayman Chemical) according to the manufacturer's protocol. At 24 h after infectious blood meal, individual female mosquitoes were stored in 100 μ l of 100% methanol at -80°C . The mosquito whole body was homogenized and kept at 4°C for 30 min before centrifugation (10,000 $\times g$, 10 min). The supernatant was transferred to a new 1.5-ml Eppendorf tube, and the solvent was removed by centrifugation at reduced pressure. The extracted total ecdysteroids were redissolved in 50 μ l of EIA buffer, and loaded on the 96-well strip plate precoated with mouse anti-rabbit IgG (Cayman Chemical). Samples in duplicate were incubated with 50 μ l tracer and 50 μ l 20E antiserum overnight at 4°C and then developed with 200 μ l Ellman's Reagent for 90–120 min. Absorbance was measured by a BioTek Synergy Mx microplate reader at 412 nm.

20E microinjection

2 h after mosquitoes took a blood meal, 20E (CAS 5289-74-7, Santa Cruz Biotechnology, sc-202407) was microinjected into each mosquito using a Nanoject II Auto-Nanoliter Injector (Drummond). At 24 h after blood feeding, the fat bodies from five mosquitoes were dissected into RLT buffer, and total RNA was extracted to analyze the *Vg* expression by quantitative RT-PCR (RT-qPCR). *P. berghei* oocyst number and infection prevalence in 20E-injected mosquitoes were examined at 8 dpi as mentioned above.

Primers

All primers used in this study are listed in Table S1.

Statistical analysis

All data analysis, graphing, and statistics were performed in Prism (v7.0, GraphPad Software).

Online supplemental material

Fig. S1 shows a schematic describing the experimental crosses. Fig. S2 reveals the influence of *mosGILT* disruption on pupation time and male reproduction system, in addition to *mosGILT* expression in WT *A. gambiae* at larval, pupal, and adult stages. Fig. S3 depicts representative images of *P. berghei* parasites in the midguts of siblings and *mosGILT* mutants. Fig. S4 demonstrates the restoration of *Vg* expression in *mosGILT* mutants by 20E injection. Fig. S5 shows that *mosGILT* silencing does not alter *Vg* expression and *P. berghei* infection in WT mosquitoes that have normal ovaries. Table S1 lists primers used in this study.

Acknowledgments

We thank Kathleen DePonte, Mingjie Wu, Alfred Jiang, and Dr. Akash Gupta for their assistance and laboratory support. We thank the Johns Hopkins Malaria Research Institute insectary

and parasitology core facilities for providing mosquito rearing resources and *P. falciparum* gametocyte cultures. We thank Dr. Elena A. Levashina for rabbit anti-TEP1 and rabbit anti-PPO2 antibodies. We thank Dr. Eric Marois for fruitful discussion on the CRISPR/Cas9 technology and Dr. Yue Li for helpful discussions on the manuscript.

This work was supported by funding from the Howard Hughes Medical Institute and the National Institutes of Health (138949).

The authors declare no competing financial interests.

Author contributions: J. Yang, T.R. Schleicher, Y. Dong, H.B. Park, J. Lan, P. Cresswell, J. Crawford, G. Dimopoulos, and E. Fikrig designed, performed, and analyzed experiments. Y. Dong performed the embryo microinjections, generated the *mosGILT*-gRNA-expressing mosquito line, and performed the *P. falciparum* infection studies. H.B. Park helped with the detection of mosquito hormones. J. Lan helped with the maintenance of mosquito colonies, mosquito crossings, and genotyping. The paper was written by J. Yang, T.R. Schleicher, and E. Fikrig. All authors discussed the results and commented on the manuscript.

Submitted: 15 April 2019

Revised: 6 August 2019

Accepted: 25 September 2019

References

- Angleró-Rodríguez, Y.I., B.J. Blumberg, Y. Dong, S.L. Sandiford, A. Pike, A.M. Clayton, and G. Dimopoulos. 2016. A natural *Anopheles*-associated *Penicillium chrysogenum* enhances mosquito susceptibility to *Plasmodium* infection. *Sci. Rep.* 6:34084. <https://doi.org/10.1038/srep34084>
- Attardo, G.M., I.A. Hansen, and A.S. Raikhel. 2005. Nutritional regulation of vitellogenesis in mosquitoes: implications for anautogeny. *Insect Biochem. Mol. Biol.* 35:661–675. <https://doi.org/10.1016/j.ibmb.2005.02.013>
- Baldini, F., P. Gabrieli, A. South, C. Valim, F. Mancini, and F. Catteruccia. 2013. The interaction between a sexually transferred steroid hormone and a female protein regulates oogenesis in the malaria mosquito *Anopheles gambiae*. *PLoS Biol.* 11:e1001695. <https://doi.org/10.1371/journal.pbio.1001695>
- Blandin, S., and E.A. Levashina. 2004. Mosquito immune responses against malaria parasites. *Curr. Opin. Immunol.* 16:16–20. <https://doi.org/10.1016/j.coi.2003.11.010>
- Blandin, S., S.H. Shiao, L.F. Moita, C.J. Janse, A.P. Waters, F.C. Kafatos, and E.A. Levashina. 2004. Complement-like protein TEP1 is a determinant of vectorial capacity in the malaria vector *Anopheles gambiae*. *Cell.* 116: 661–670. [https://doi.org/10.1016/S0092-8674\(04\)00173-4](https://doi.org/10.1016/S0092-8674(04)00173-4)
- Blandin, S.A., E. Marois, and E.A. Levashina. 2008. Antimalarial responses in *Anopheles gambiae*: from a complement-like protein to a complement-like pathway. *Cell Host Microbe.* 3:364–374. <https://doi.org/10.1016/j.chom.2008.05.007>
- Christophides, G.K., E. Zdobnov, C. Barillas-Mury, E. Birney, S. Blandin, C. Blass, P.T. Brey, F.H. Collins, A. Danielli, G. Dimopoulos, et al. 2002. Immunity-related genes and gene families in *Anopheles gambiae*. *Science.* 298:159–165. <https://doi.org/10.1126/science.1077136>
- Collins, F.H., R.K. Sakai, K.D. Vernick, S. Paskewitz, D.C. Seeley, L.H. Miller, W.E. Collins, C.C. Campbell, and R.W. Gwadz. 1986. Genetic selection of a *Plasmodium*-refractory strain of the malaria vector *Anopheles gambiae*. *Science.* 234:607–610. <https://doi.org/10.1126/science.3532325>
- Dimopoulos, G., D. Seeley, A. Wolf, and F.C. Kafatos. 1998. Malaria infection of the mosquito *Anopheles gambiae* activates immune-responsive genes during critical transition stages of the parasite life cycle. *EMBO J.* 17: 6115–6123. <https://doi.org/10.1093/emboj/17.21.6115>
- Dimopoulos, G., G.K. Christophides, S. Meister, J. Schultz, K.P. White, C. Barillas-Mury, and F.C. Kafatos. 2002. Genome expression analysis of *Anopheles gambiae*: responses to injury, bacterial challenge, and malaria infection. *Proc. Natl. Acad. Sci. USA.* 99:8814–8819. <https://doi.org/10.1073/pnas.092274999>
- Dong, Y., R. Aguilar, Z. Xi, E. Warr, E. Mongin, and G. Dimopoulos. 2006. *Anopheles gambiae* immune responses to human and rodent *Plasmodium* parasite species. *PLoS Pathog.* 2:e52. <https://doi.org/10.1371/journal.ppat.0020052>
- Dong, Y., M.L. Simões, E. Marois, and G. Dimopoulos. 2018. CRISPR/Cas9-mediated gene knockout of *Anopheles gambiae* *FREPI* suppresses malaria parasite infection. *PLoS Pathog.* 14:e1006898. <https://doi.org/10.1371/journal.ppat.1006898>
- Fraiture, M., R.H.G. Baxter, S. Steinert, Y. Chelliah, C. Frolet, W. Quispe-Tintaya, J.A. Hoffmann, S.A. Blandin, and E.A. Levashina. 2009. Two mosquito LRR proteins function as complement control factors in the TEP1-mediated killing of *Plasmodium*. *Cell Host Microbe.* 5:273–284. <https://doi.org/10.1016/j.chom.2009.01.005>
- Gabrieli, P., E.G. Kakani, S.N. Mitchell, E. Mameli, E.J. Want, A. Mariezcurrera Anton, A. Serrao, F. Baldini, and F. Catteruccia. 2014. Sexual transfer of the steroid hormone 20E induces the postmating switch in *Anopheles gambiae*. *Proc. Natl. Acad. Sci. USA.* 111:16353–16358. <https://doi.org/10.1073/pnas.1410488111>
- Gantz, V.M., N. Jasinskiene, O. Tatarenkova, A. Fazekas, V.M. Macias, E. Bier, and A.A. James. 2015. Highly efficient Cas9-mediated gene drive for population modification of the malaria vector mosquito *Anopheles stephensi*. *Proc. Natl. Acad. Sci. USA.* 112:E6736–E6743. <https://doi.org/10.1073/pnas.1521077112>
- Ghosh, A., M.J. Edwards, and M. Jacobs-Lorena. 2000. The journey of the malaria parasite in the mosquito: hopes for the new century. *Parasitol. Today (Regul. Ed.)*. 16:196–201. [https://doi.org/10.1016/S0169-4758\(99\)01626-9](https://doi.org/10.1016/S0169-4758(99)01626-9)
- Hagedorn, H.H., J.D. O'Connor, M.S. Fuchs, B. Sage, D.A. Schlaeger, and M.K. Bohm. 1975. The ovary as a source of alpha-ecdysone in an adult mosquito. *Proc. Natl. Acad. Sci. USA.* 72:3255–3259. <https://doi.org/10.1073/pnas.72.8.3255>
- Hammond, A., R. Galizi, K. Kyrou, A. Simoni, C. Siniscalchi, D. Katsanos, M. Gribble, D. Baker, E. Marois, S. Russell, et al. 2016. A CRISPR-Cas9 gene drive system targeting female reproduction in the malaria mosquito vector *Anopheles gambiae*. *Nat. Biotechnol.* 34:78–83. <https://doi.org/10.1038/nbt.3439>
- Kokoza, V.A., D. Martin, M.J. Mienaltowski, A. Ahmed, C.M. Morton, and A.S. Raikhel. 2001. Transcriptional regulation of the mosquito vitellogenin gene via a blood meal-triggered cascade. *Gene.* 274:47–65. [https://doi.org/10.1016/S0378-1119\(01\)00602-3](https://doi.org/10.1016/S0378-1119(01)00602-3)
- Lea, A.O. 1982. Artfactual stimulation of vitellogenesis in *Aedes aegypti* by 20-hydroxyecdysone. *J. Insect Physiol.* 28:173–176. [https://doi.org/10.1016/0022-1910\(82\)90125-1](https://doi.org/10.1016/0022-1910(82)90125-1)
- Levashina, E.A., L.F. Moita, S. Blandin, G. Vriend, M. Lagueux, and F.C. Kafatos. 2001. Conserved role of a complement-like protein in phagocytosis revealed by dsRNA knockout in cultured cells of the mosquito, *Anopheles gambiae*. *Cell.* 104:709–718. [https://doi.org/10.1016/S0092-8674\(01\)00267-7](https://doi.org/10.1016/S0092-8674(01)00267-7)
- Livak, K.J., and T.D. Schmittgen. 2001. Analysis of relative gene expression data using real-time quantitative PCR and the 2^{-ΔΔC_T} (ΔΔC_T) Method. *Methods.* 25:402–408. <https://doi.org/10.1006/meth.2001.1262>
- Mendes, A.M., T. Schlegelmilch, A. Cohuet, P. Awono-Ambene, M. De Iorio, D. Fontenille, I. Morlais, G.K. Christophides, F.C. Kafatos, and D. Vlachou. 2008. Conserved mosquito/parasite interactions affect development of *Plasmodium falciparum* in Africa. *PLoS Pathog.* 4:e1000069. <https://doi.org/10.1371/journal.ppat.1000069>
- Meredith, J.M., A. Underhill, C.C. McArthur, and P. Eggleston. 2013. Next-generation site-directed transgenesis in the malaria vector mosquito *Anopheles gambiae*: self-docking strains expressing germline-specific phiC31 integrase. *PLoS One.* 8:e59264. <https://doi.org/10.1371/journal.pone.0059264>
- Mianné, J., G.F. Codner, A. Caulder, R. Fell, M. Hutchison, R. King, M.E. Stewart, S. Wells, and L. Teboul. 2017. Analysing the outcome of CRISPR-aided genome editing in embryos: Screening, genotyping and quality control. *Methods.* 121–122:68–76. <https://doi.org/10.1016/j.ymeth.2017.03.016>
- Michel, K., A. Budd, S. Pinto, T.J. Gibson, and F.C. Kafatos. 2005. *Anopheles gambiae* SRPN2 facilitates midgut invasion by the malaria parasite *Plasmodium berghei*. *EMBO Rep.* 6:891–897. <https://doi.org/10.1038/sj.embor.7400478>
- Osta, M.A., G.K. Christophides, and F.C. Kafatos. 2004. Effects of mosquito genes on *Plasmodium* development. *Science.* 303:2030–2032. <https://doi.org/10.1126/science.1091789>

- Papathanos, P.A., N. Windbichler, M. Menichelli, A. Burt, and A. Crisanti. 2009. The vasa regulatory region mediates germline expression and maternal transmission of proteins in the malaria mosquito *Anopheles gambiae*: a versatile tool for genetic control strategies. *BMC Mol. Biol.* 10: 65. <https://doi.org/10.1186/1471-2199-10-65>
- Pike, A., Y. Dong, N.B. Dizaji, A. Gacita, E.F. Mongodin, and G. Dimopoulos. 2017. Changes in the microbiota cause genetically modified *Anopheles* to spread in a population. *Science*. 357:1396–1399. <https://doi.org/10.1126/science.aak9691>
- Pondeville, E., A. Maria, J.C. Jacques, C. Bourgoquin, and C. Dauphin-Villemanant. 2008. *Anopheles gambiae* males produce and transfer the vitellogenin steroid hormone 20-hydroxyecdysone to females during mating. *Proc. Natl. Acad. Sci. USA*. 105:19631–19636. <https://doi.org/10.1073/pnas.0809264105>
- Port, F., H.M. Chen, T. Lee, and S.L. Bullock. 2014. Optimized CRISPR/Cas tools for efficient germline and somatic genome engineering in *Drosophila*. *Proc. Natl. Acad. Sci. USA*. 111:E2967–E2976. <https://doi.org/10.1073/pnas.1405500111>
- Povelones, M., R.M. Waterhouse, F.C. Kafatos, and G.K. Christophides. 2009. Leucine-rich repeat protein complex activates mosquito complement in defense against *Plasmodium* parasites. *Science*. 324:258–261. <https://doi.org/10.1126/science.1171400>
- Povelones, M., L.M. Upton, K.A. Sala, and G.K. Christophides. 2011. Structure-function analysis of the *Anopheles gambiae* LRIM1/APLIC complex and its interaction with complement C3-like protein TEPI. *PLoS Pathog.* 7: e1002023. <https://doi.org/10.1371/journal.ppat.1002023>
- Povelones, M., L. Bhagavatula, H. Yassine, L.A. Tan, L.M. Upton, M.A. Osta, and G.K. Christophides. 2013. The CLIP-domain serine protease homolog SPCLIP1 regulates complement recruitment to microbial surfaces in the malaria mosquito *Anopheles gambiae*. *PLoS Pathog.* 9: e1003623. <https://doi.org/10.1371/journal.ppat.1003623>
- Raikhel, A.S., M.R. Brown, and X. Belles. 2005. Hormonal control of reproductive processes. In *Comprehensive Molecular Insect Science*. L.I. Gilbert, K. Iatrou, and S.S. Gill, editors. Elsevier, Oxford, UK. pp. 433–491. <https://doi.org/10.1016/B0-44-451924-6/00040-5>
- Riehle, M.M., K. Markianos, O. Niaré, J. Xu, J. Li, A.M. Touré, B. Podiougou, F. Oduol, S. Diawara, M. Diallo, et al. 2006. Natural malaria infection in *Anopheles gambiae* is regulated by a single genomic control region. *Science*. 312:577–579. <https://doi.org/10.1126/science.1124153>
- Riehle, M.M., J. Xu, B.P. Lazzaro, S.M. Rottschaefer, B. Coulibaly, M. Sacko, O. Niare, I. Morlais, S.F. Traore, and K.D. Vernick. 2008. *Anopheles gambiae* APL1 is a family of variable LRR proteins required for Rel1-mediated protection from the malaria parasite, *Plasmodium berghei*. *PLoS One*. 3: e3672. <https://doi.org/10.1371/journal.pone.0003672>
- Rono, M.K., M.M. Whitten, M. Oulad-Abdelghani, E.A. Levashina, and E. Marois. 2010. The major yolk protein vitellogenin interferes with the anti-*plasmodium* response in the malaria mosquito *Anopheles gambiae*. *PLoS Biol.* 8: e1000434. <https://doi.org/10.1371/journal.pbio.1000434>
- Schleicher, T.R., J. Yang, M. Freudzon, A. Rembisz, S. Craft, M. Hamilton, M. Graham, G. Mlambo, A.K. Tripathi, Y. Li, et al. 2018. A mosquito salivary gland protein partially inhibits *Plasmodium* sporozoite cell traversal and transmission. *Nat. Commun.* 9:2908. <https://doi.org/10.1038/s41467-018-05374-3>
- Schwenke, R.A., B.P. Lazzaro, and M.F. Wolfner. 2016. Reproduction-immunity trade-offs in insects. *Annu. Rev. Entomol.* 61:239–256. <https://doi.org/10.1146/annurev-ento-010715-023924>
- Simões, M.L., G. Mlambo, A. Tripathi, Y. Dong, and G. Dimopoulos. 2017. Immune regulation of *Plasmodium* is *Anopheles* species specific and infection intensity dependent. *MBio*. 8: e01631–e17. <https://doi.org/10.1128/mBio.01631-17>
- Simões, M.L., E.P. Caragata, and G. Dimopoulos. 2018. Diverse host and restriction factors regulate mosquito-pathogen interactions. *Trends Parasitol.* 34:603–616. <https://doi.org/10.1016/j.pt.2018.04.011>
- Sinden, R.E. 2002. Molecular interactions between *Plasmodium* and its insect vectors. *Cell. Microbiol.* 4:713–724. <https://doi.org/10.1046/j.1462-5822.2002.00229.x>
- Song, Y., Y. Xu, M. Liang, Y. Zhang, M. Chen, J. Deng, and Z. Li. 2018. CRISPR/Cas9-mediated mosaic mutation of *SRY* gene induces hermaphroditism in rabbits. *Biosci. Rep.* 38: BSR20171490. <https://doi.org/10.1042/BSR20171490>
- Tazuke, S.I., C. Schulz, L. Gilboa, M. Fogarty, A.P. Mahowald, A. Guichet, A. Ephrussi, C.G. Wood, R. Lehmann, and M.T. Fuller. 2002. A germline-specific gap junction protein required for survival of differentiating early germ cells. *Development*. 129:2529–2539.
- Thailayil, J., K. Magnusson, H.C. Godfray, A. Crisanti, and F. Catteruccia. 2011. Spermless males elicit large-scale female responses to mating in the malaria mosquito *Anopheles gambiae*. *Proc. Natl. Acad. Sci. USA*. 108: 13677–13681. <https://doi.org/10.1073/pnas.1104738108>
- Trager, W., and J.B. Jensen. 1976. Human malaria parasites in continuous culture. *Science*. 193:673–675. <https://doi.org/10.1126/science.781840>
- Vlachou, D., T. Schlegelmilch, G.K. Christophides, and F.C. Kafatos. 2005. Functional genomic analysis of midgut epithelial responses in *Anopheles* during *Plasmodium* invasion. *Curr. Biol.* 15:1185–1195. <https://doi.org/10.1016/j.cub.2005.06.044>
- Volohonsky, G., O. Terenzi, J. Soichot, D.A. Naujoks, T. Nolan, N. Windbichler, D. Kapps, A.L. Smidler, A. Vittu, G. Costa, et al. 2015. Tools for *Anopheles gambiae* transgenesis. *G3 (Bethesda)*. 5:1151–1163. <https://doi.org/10.1534/g3.115.016808>
- Volohonsky, G., A.K. Hopp, M. Saenger, J. Soichot, H. Scholze, J. Boch, S.A. Blandin, and E. Marois. 2017. Transgenic expression of the anti-parasitic factor TEPI in the malaria mosquito *Anopheles gambiae*. *PLoS Pathog.* 13: e1006113. <https://doi.org/10.1371/journal.ppat.1006113>
- Werling, K., W.R. Shaw, M.A. Itoe, K.A. Westervelt, P. Marcenac, D.G. Paton, D. Peng, N. Singh, A.L. Smidler, A. South, et al. 2019. Steroid hormone function controls non-competitive *Plasmodium* development in *Anopheles*. *Cell*. 177:315–325.e14. <https://doi.org/10.1016/j.cell.2019.02.036>
- World Health Organization. 2017. World Malaria Report. Available at: <https://apps.who.int/iris/bitstream/handle/10665/259492/9789241565523-eng.pdf> (accessed August 6, 2018).

Supplemental material

Yang et al., <https://doi.org/10.1084/jem.20190682>

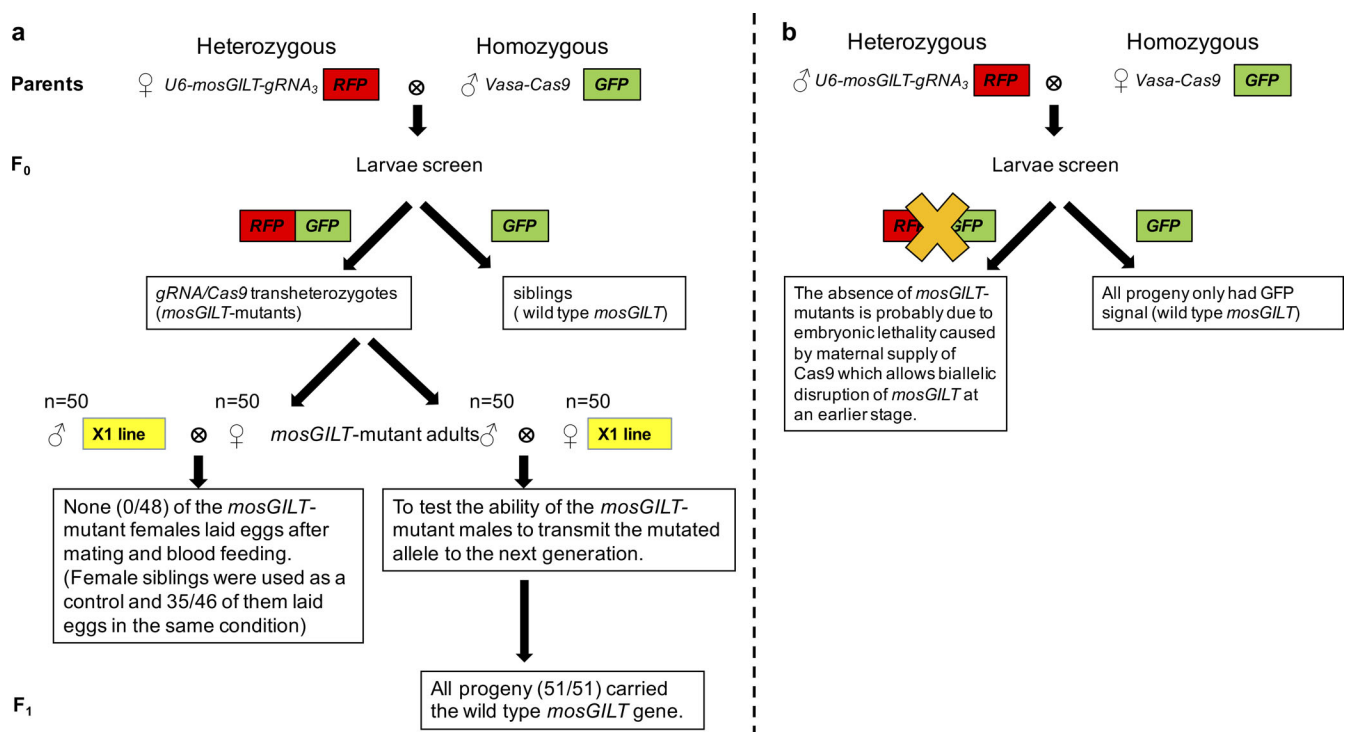


Figure S1. **Schematic for experimental crosses. (a)** Generation of *mosGILT* mutants and analysis of their ability to pass down the mutations to the next generation. Females of the *A. gambiae* line heterozygous for *mosGILT-gRNA₃/RFP* were crossed with males of the *A. gambiae* line homozygous for *Cas9/GFP*. Their progeny were separated into two groups by screening the fluorescent markers in the larvae: the founder animals (F₀) with both the RFP and GFP signals were *mosGILT* mutants (or *gRNA/Cas9* transheterozygotes), which carried the *mosGILT* mutations; the other ones with only GFP signals were WT siblings. When 50 *mosGILT* mutant females were outcrossed with 50 X1 males, none of the surviving *mosGILT* mutant females (0/48) laid eggs after mating and blood feeding. 50 WT female siblings were used as a control and 35/46 of the surviving WT females laid eggs in the same condition. When 50 *mosGILT* mutant males were outcrossed with 50 X1 females, 51 progeny were genotyped and all of them (51/51) carried only the WT *mosGILT* alleles. **(b)** *mosGILT* mutants cannot be obtained from the reciprocal cross using the males heterozygous for *mosGILT-gRNA₃/RFP* and females homozygous for *Cas9/GFP*. All the progeny of this cross were WT siblings as they showed only GFP signals. The maternal supply of Cas9 could allow an earlier biallelic disruption of *mosGILT*, leading to embryonic lethality.

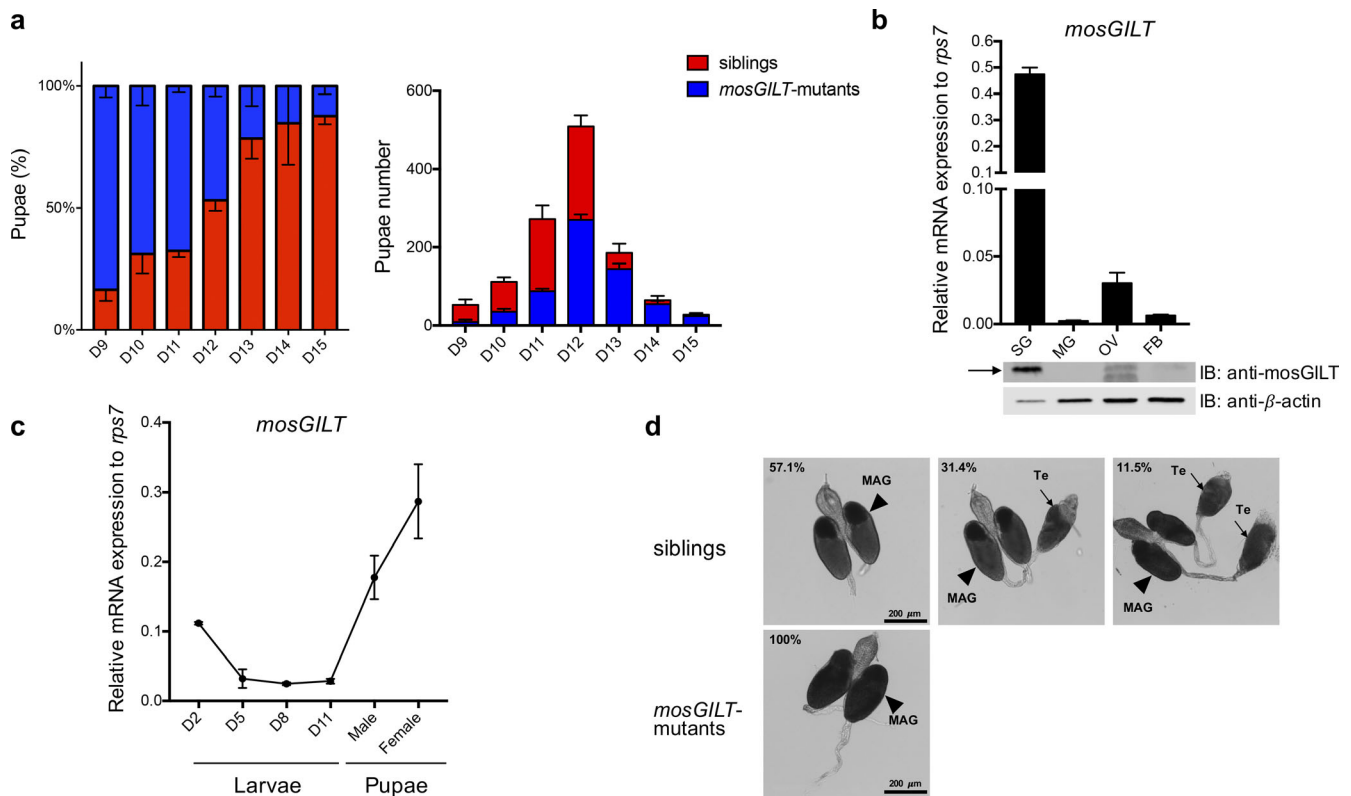


Figure S2. **Additional *mosGILT* mutant phenotypes and *mosGILT* expression profile.** (a) Pupation time was slightly delayed in *mosGILT* mutants compared with siblings. The proportion (left) and the number (right) of pupae collected from each group are shown on a daily basis starting at day 9 after hatching. (b) Expression levels of *mosGILT* mRNA (upper panel) and protein (lower panel) in the SG, midguts (MG), ovaries (OV), and fat body (FB) of WT female mosquitoes. Black arrow indicates the band for *mosGILT*. (c) Transcript levels of *mosGILT* in larvae at day 2, 5, 8, and 11 after hatching and pupae. (d) Male reproductive system dissected from 7-d-old siblings and *mosGILT* mutants. Male accessory glands (MAG) and Te are indicated with arrowheads and arrows, respectively. 35 males were examined in each group, and the percentages of males displaying 0, 1, or 2 Te are shown on the upper left. All the data are representative of three independent experiments (mean \pm SD).

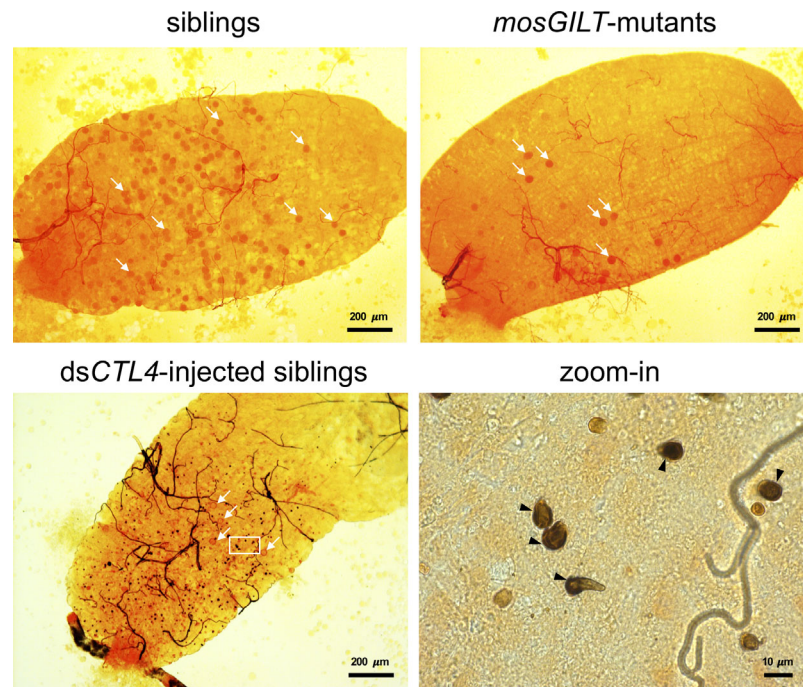


Figure S3. **Mercurochrome staining of *P. berghei*-infected midguts.** Representative images of *P. berghei*-infected midguts (8 dpi) from the infection studies demonstrated the striking decrease of developing oocysts (white arrows) in *mosGILT* mutants compared with siblings. Melanized ookinetes were not seen in both groups. Silencing of *CTL4* was used as a positive control, which triggered massive melanization of ookinetes in the midguts of siblings (scale bars, 200 μ m). The region highlighted by the white square is displayed at a higher magnification on the bottom right (scale bar, 10 μ m). Melanized ookinetes are indicated by black arrowheads.

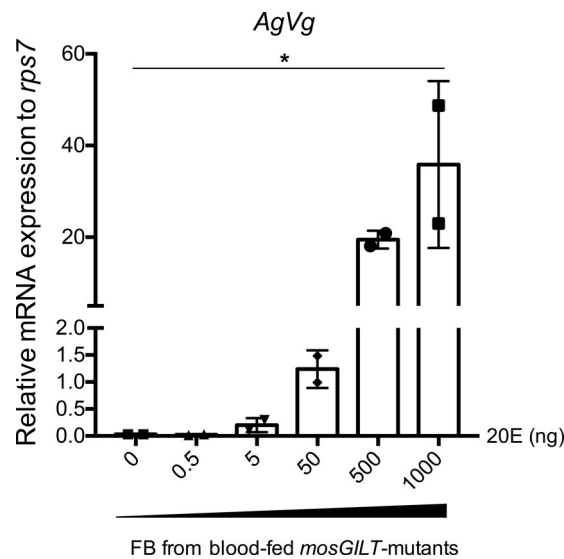


Figure S4. **A dose-dependent stimulation of *Vg* expression in *mosGILT* mutants by supplying exogenous 20E.** Transcript level of *AgVg* in the fat body of *mosGILT* mutant females injected with the indicated doses of 20E at 24 h after blood feeding. 20E was injected into mosquitoes at 2 h after blood feeding. Data are representative of three independent experiments (mean \pm SD, one-way ANOVA, *, $P < 0.05$).

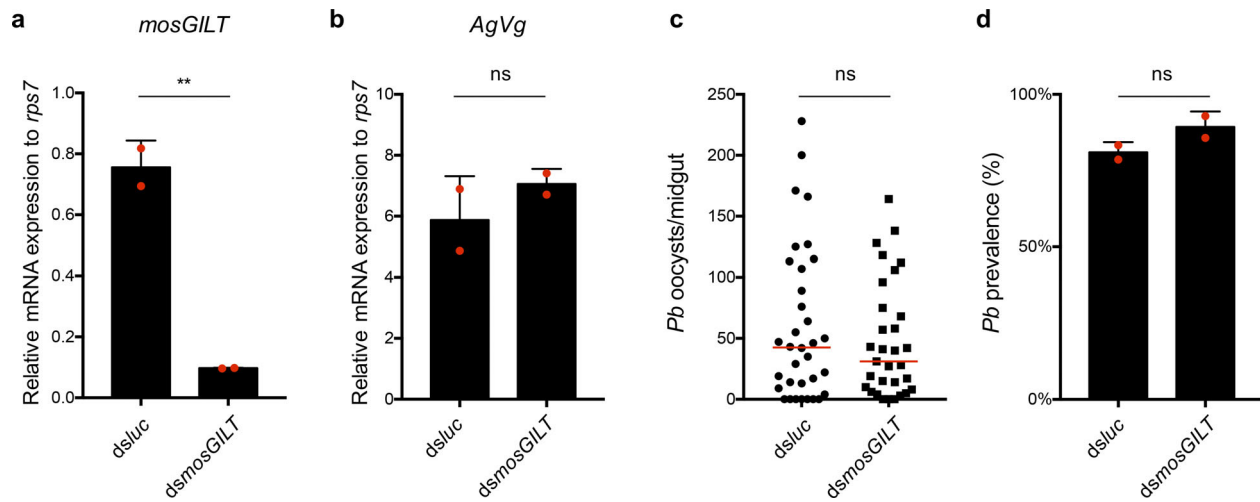


Figure S5. **Silencing of *mosGILT* in WT *A. gambiae* does not influence *Vg* expression and *P. berghei* infection.** (a) *mosGILT* knockdown efficiency in the injected X1 females was validated by RT-qPCR of SG cells 4 d after dsRNA injection. Data are representative of more than three experiments (each dot represents five mosquitoes, mean \pm SD, unpaired t test, **, $P < 0.01$). (b) Transcript levels of *AgVg* in the fat body of *dsluc* or *dsmosGILT* injected females 24 h after feeding on *P. berghei*-infected mice. Data represent duplicate experiments from two experiments (each dot represents five mosquitoes, mean \pm SD, unpaired t test, ns, not significant). (c and d) *P. berghei* oocyst number (c) and infection prevalence (d) in the midgut 8 dpi. Each dot in panel c represents the oocyst number in one mosquito midgut (data pooled from two independent experiments, X1 *dsluc* $n = 34$, X1 *dsmosGILT* $n = 31$, Mann-Whitney test, ns, not significant). The horizontal lines (red) indicate the medians. Each dot in panel d represents one independent experiment (mean \pm SD, Fisher's exact test, ns, not significant).

Table S1 is provided online as a separate Excel file and lists primer information used in this study.